

EFFECTS OF RELAXATION OF A  
CORE ON A WOUND ROLL

By

JEFFREY SCOTT HENNING

Bachelor of Science

Oklahoma State University

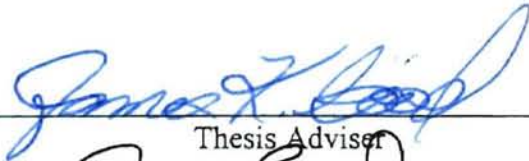
Stillwater, Oklahoma

1995

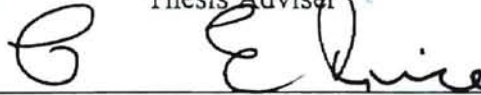
Submitted to the Faculty of the  
Graduate College of the  
Oklahoma State University  
in partial fulfillment of  
the requirements for  
the Degree of  
MASTER OF SCIENCE  
May 1997

EFFECTS OF RELAXATION OF A  
CORE ON A WOUND ROLL

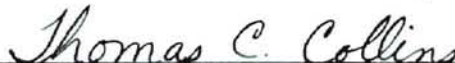
Thesis Approved:

  
\_\_\_\_\_

Thesis Adviser

  
\_\_\_\_\_

  
\_\_\_\_\_

  
\_\_\_\_\_

Dean of the Graduate College

## ACKNOWLEDGMENTS

I wish to thank Dr. James K. Good, Professor, Mechanical and Aerospace Engineering and my advisor. His guidance throughout my research has been invaluable.

Gratitude is also extended to Charles Johnson, Sonoco, Inc., for his technical support and for providing materials. His moral support is also greatly appreciated.

Thanks must also go to Ron Markum and Robert Taylor of the OSU Web Handling Research Center for their expertise.

For her generous patience, support and love I thank my wife, Susie.

## TABLE OF CONTENTS

Chapter	Page
I. INTRODUCTION .....	1
II. LITERATURE REVIEW .....	3
Elastic Core Model .....	3
Hakiel's Model.....	3
Thermal Analysis .....	8
Tube Testing Device .....	9
III. FINDING AN EXPERIMENTAL RELAXATION FUNCTION.....	11
Pressure Vessel Design .....	11
Deflection Measurement .....	13
Miscellaneous Instrumentation .....	14
Data Acquisition .....	15
Experimental Procedure .....	16
Data Analysis .....	17
IV. ROLL MODEL.....	27
Computer Model .....	30
V. MODEL VERIFICATION .....	33
Roll Testing.....	35
VI. CONCLUSIONS .....	43
VII. FUTURE WORK .....	44
REFERENCES .....	45

## LIST OF FIGURES

Figure	Page
1. Pressure Vessel.....	13
2. Pressure Vessel Layout .....	14
3. Strain Data for Core #1	
a. Strain Data for Core #1 at 100 psi.....	18
b. Strain Data for Core #1 at 150 psi.....	18
c. Strain Data for Core #1 at 200 psi.....	19
4. Average Strain Data for Core #1 .....	20
5. Normalized Creep Data for Core #1.....	20
6. Creep Function Plot of Core #1.....	21
7. Strain Data for Core #2	
a. Strain Data for Core #2 at 100 psi.....	22
b. Strain Data for Core #2 at 150 psi.....	23
c. Strain Data for Core #2 at 200 psi.....	23
8. Average Strain Data for Core #2 .....	24
9. Normalized Creep Plot for Core #2.....	24
10. Creep Function Plot of Core #2.....	25
11. Flow Chart .....	32
12. Radial Pressure Through Winding .....	34
13. Core Pressure Through Winding .....	34
14. Die Set .....	37

15. Push Test Set up .....	37
16. Roll #4 Push Force .....	39
17. Role #4 Radial Pressure.....	40
18. Roll # 5 Push Force .....	41
19. Roll #5 Radial Pressure .....	42

## NOMENCLATURE

$b$	web thickness
$E_c$	core modulus of elasticity
$E_r$	radial modulus of elasticity
$E_t$	tangential modulus of elasticity
$F$	punch force
$h$	incremental change in central difference approximation
$J$	core relaxation function
$J_0, J_1, T_1, J_2, T_2$	coefficients in the relaxation function
$K'$	effective gage factor of strain gage
$N$	interlayer force
$P$	interlayer pressure
$R'_A$	effective resistance of arm shunted (ohms)
$R_{cal}$	resistance of calibration resistor (ohms)
$r$	radius
$t$	time
$T_w$	winding tension stress
$w$	web width

$\delta T$	incremental change in tension stress
$\epsilon_{cal}$	simulated strain
$\epsilon_r$	radial strain
$\epsilon_t$	tangential strain
$\nu_r$	radial Poison's ratio
$\nu_{tr}$	tangential Poison's ratio
$\sigma_r$	radial stress
$\sigma_t$	tangential stress



## CHAPTER I

### INTRODUCTION

Many materials used in the world today originate through a web handling process. Thin plastic films, paper, cotton fibers, and thin metals are manufactured in continuous strips called webs. For convenience, web material is wound on to a roll where it can be easily transported and stored. The web is wound on to cores made of materials such as: composite fiber, plastic, aluminum or steel. The core is a cylindrical hollow shell. It is hollow for ease of mounting the roll on to the appropriate web handling equipment. For economic reasons, the core used for a specific web has the minimum required properties, such as strength and weight. Industry desires a disposable core so the core will not have to be returned to the manufacturing plant. With these requirements, it is important to have a process for finding the best core for the specific web.

In web handling processes, it is important to maintain roll integrity. Extreme stresses within the roll cause defects to occur, such as wrinkling or starring, thus yielding the damaged portion of the roll unusable. Also, inappropriate stresses can cause the roll to separate from the core. If that occurs, problems arise in unwinding the roll, because tension is applied to the core during unwinding. This results in an unusable roll. To ensure roll integrity, an effort has been made to develop winding models which predict the stresses within the roll.

Winding models incorporate web material properties, core properties and winding techniques. From the results of winding models, criteria can be generated to determine whether flaws will occur. These models reflect the dynamic effects of the winding

process. Very few models reflect how the roll will act with environmental or time effects. It has been noted that, at times, a roll has developed defects days after it has been wound even without a temperature change. This must be due to an effect that occurred after the dynamic winding response.

Current models assume the core is an elastic material. It is often a viscoelastic material. A viscoelastic material is defined as a material that exhibits an elastic strain upon loading, then a slow and continuous increase in strain through time at a decreasing rate.[1] When the loading is removed, the initial elastic strain is immediately recovered and then a slow continuous decrease in strain occurs. The slow continuous increase in strain under constant stress is called creep. This viscoelastic property of a paperboard core is explored in this paper in order to explain how flaws develop through time in a wound roll.

The study begins with a development of a roll model that begins with the winding process and ends at a set time later. Typically, roll models consist of second order differential equations with two boundary conditions. One boundary condition is at the outside radius of the roll, which is influenced by the winding tension. The second boundary condition is at the roll-core interface in which a core deformation dominates. An empirical function will be developed to model the rate of radial deformation of the core due to roll stress. The roll model will be solved analytically using a finite difference approximation. Finally, experimental verification of the model is presented.

## CHAPTER II

### Literature Review

#### Elastic Core Model

An elastic core model was developed to predict stresses and strains, for spiral paper tubes loaded axisymmetrically by Gerhardt, of Sonoco Product Co. [2]. This model did not assume the core to be isotropic or any stress distribution through the core wall. Paper, however, was assumed to be a linear elastic material.

Experimentation verified the elastic core model. Some results are as followed. One, paperboard laminates exhibit nonlinear stress-strain behavior. Two, hoop stress dominates all other stress components and it was not constant across the tube wall. Three, a stress concentration occurred at the outer wall of the tube and remained constant as the tube thickness increased.

#### Hakiel's Model

The viscoelastic properties of the core affect the quality of a wound roll. Core creep, induced by stresses exerted by the wound roll, plays a major part in the quality of the wound roll. The wound roll stresses must be known.

Hakiel developed a nonlinear orthotropic hoop model for center wound rolls. [3] The roll stresses are calculated by solving a second order differential equation with two boundary conditions. Since the equation is nonlinear, numeric approximations are used.

The following assumptions are made in Hakiel's model:

1. The winding roll is a geometrically perfect cylinder with the web having uniform width, thickness, and length.
2. The roll is a collection of concentric hoops. Winding is modeled by the addition of tensioned hoops. Roll properties remain constant.
3. The roll is an orthotropic, elastic cylinder with linear-elastic behavior in the circumferential direction and non-linear-elastic behavior in the radial direction. The radial modulus of elasticity is known and varies as a function of radial stress.
4. The stresses within the roll are a function of radial position only.
5. The roll is under a plane stress condition and axial stresses are equal to zero.

Hakiel uses three basic stress strain equations to support his model.

1. The equilibrium equation for plane stress in cylindrical coordinates in the absence of shear:

$$r\left(\frac{\partial\sigma_r}{\partial r}\right) - \sigma_t + \sigma_r = 0 \quad (2.1)$$

2. The linear orthotropic constitutive equations:

$$\varepsilon_r = \frac{\sigma_r}{E_r} - \left(\frac{\nu_{rt}}{E_t}\right)\sigma_t \quad (2.2a)$$

$$\varepsilon_t = \frac{\sigma_t}{E_t} - \left(\frac{\nu_{tr}}{E_r}\right)\sigma_r \quad (2.2b)$$

3. The strain compatibility equation:

$$r \left( \frac{\partial \varepsilon_t}{\partial r} \right) + \varepsilon_t - \varepsilon_r = 0 \quad (2.3)$$

The model begins by solving the equilibrium equation (2.1) for  $\sigma_r$  and substituting it into the constitutive equations (2.2a,b).

$$\begin{aligned} \varepsilon_r &= \frac{\sigma_r}{E_r} - \frac{\nu_{rt}}{E_t} \left( r \frac{\partial \sigma_r}{\partial r} + \sigma_r \right) \\ \text{and} \\ \varepsilon_t &= \frac{1}{E_t} \left( r \frac{\partial \sigma_r}{\partial r} + \sigma_r \right) - \left( \frac{\nu_{tr}}{E_r} \right) \sigma_r \end{aligned} \quad (2.4)$$

Then, substituting these two equations into the strain compatibility equation (2.3)

$$r \left[ \frac{\partial \left( \frac{1}{E_t} \left( r \frac{\partial \sigma_r}{\partial r} + \sigma_r \right) - \left( \frac{\nu_{tr}}{E_r} \right) \sigma_r \right)}{\partial r} \right] + \frac{1}{E_t} \left( r \frac{\partial \sigma_r}{\partial r} + \sigma_r \right) - \left( \frac{\nu_{tr}}{E_r} \right) \sigma_r - \frac{\sigma_r}{E_r} - \frac{\nu_{rt}}{E_t} \left( r \frac{\partial \sigma_r}{\partial r} + \sigma_r \right) = 0 \quad (2.5)$$

Solving and utilizing Maxwell's relationship :  $\frac{\nu_{tr}}{E_r} = \frac{\nu_{rt}}{E_t}$  yields:

$$r^2 \frac{\partial^2 \sigma_r}{\partial r^2} + 3r \frac{\partial \sigma_r}{\partial r} + \left( 1 - \frac{E_t}{E_r} \right) \sigma_r = 0 \quad (2.6)$$

Hakiel's second order differential equation is the governing equation in the winding model. To solve the equation, two boundary conditions are required. The first boundary condition, at the core- roll interface, is obtained by equating the radial deformation of the first wound on layer (2.7) and outside deformation of the core (2.8).

$$u(1) = \left( \frac{1}{E_t} \right) (\delta T + \nu \delta \sigma_r) \quad (2.7)$$

$$u(1) = -\frac{\delta\sigma_r(1)}{E_c} \quad (2.8)$$

Where the  $\delta$  indicates incremental changes in the variable.

Substituting the deformation equations (2.7)(2.8) in the equilibrium equation (2.1) yields the first boundary condition.

$$\frac{\partial\delta\sigma_r}{\partial r}\Big|_{r=1} = \left(\frac{E_t}{E_c} - 1 + \nu\right)\delta\sigma_r\Big|_{r=1} \quad (2.9)$$

The second boundary condition, at the outside of the winding roll, is found by assuming the incremental winding on of the last lap is equal to the hoop stress of that lap.

$$\delta\sigma_r\Big|_{r=s} = \left(\frac{Tw\Big|_{r=s}}{s}\right)b \quad (2.10)$$

With these two boundary conditions, a solution can be obtained for the Hakiel's governing differential equation of the elastic region of this model.

Since the model is nonlinear, the solution must be found analytically. A finite difference method with a central difference approximation of the derivatives is employed to solve the governing differential equation. The central difference approximations are as follows:

$$\frac{\partial\sigma_r}{\partial r} = \frac{\sigma_r(i+1) - \sigma_r(i)}{h} \quad (2.11a)$$

$$\frac{\partial^2\sigma_r}{\partial r^2} = \frac{\sigma_r(i-1) - 2\sigma_r(i) + \sigma_r(i+1)}{h^2} \quad (2.11b)$$

Substituting the approximations into the governing differential equation (2.6) and combing variables yields:

$$\left(\frac{r^2}{h^2} - \frac{3r}{2h}\right)\sigma_r(i-1) + \left(\frac{-2r^2}{h^2} + 1 - \frac{E_t}{E_r}\right)\sigma_r(i) + \left(\frac{r^2}{h^2} + \frac{3r}{2h}\right)\sigma_r(i+1) = 0 \quad (2.12)$$

Where (i) is the current lap and h is the incremental step size or web thickness.

Substituting the approximations into the dynamic boundary conditions (2.9)(2.10) and collecting terms they become:

$$\delta\sigma_r(i+1) - \left[\frac{1}{h}\left(h - \frac{E_t}{E_c} - 1 + \nu\right)\right]\delta\sigma_r(i) = 0$$

and

$$\delta\sigma_r(i) = \left(\frac{Tw}{i}\right)h \quad (2.13)$$

With the governing differential equation written at all interior points (web laps) in the roll, a set of equations are formed for N-2 variables. The two boundary conditions supply the remaining two required equations. Thus, the boundary value problem has been reduced into a simultaneous set of equations. When put in matrix form, they yield a tri-diagonal system of the form:

$$[A]\{\delta\sigma_r\} = [B] \quad (2.14)$$

The system can be solved by a Gaussian elimination routine with N-2 forward and N-1 backward substitution. The incremental stresses are accumulated at each layer and added together to get the total stress at that layer. This process steps through the roll adding layer upon layer until the entire roll is analyzed.

### Thermal Analysis

One recent study by Qualls [4] investigated the effect of a temperature change upon a roll. Qualls showed that an increase in temperature increased the stresses causing

defects within the roll. This was due to expansion or contraction of both the web material and the core. Qualls modified Hakiel's wound roll model to calculate the interlayer pressures in a wound roll which is subjected to a homogeneous temperature change. The model includes coefficients of thermal expansion of the web and core. The constitutive equations become:

$$\varepsilon_r = \frac{\sigma_r}{E_r} - \left( \frac{\nu_{rt}}{E_t} \right) \sigma_t + \alpha_r \Delta T \quad (2.15a)$$

$$\varepsilon_t = \frac{\sigma_t}{E_t} - \left( \frac{\nu_{tr}}{E_r} \right) \sigma_r + \alpha_t \Delta T \quad (2.15b)$$

where  $\alpha_r$  is the radial coefficient of thermal expansion of the web

$\alpha_t$  is the tangential coefficient of thermal expansion of the web

$\Delta T$  is the temperature change

Solving the model in a similar method as Hakiel, the second order differential governing equation becomes:

$$r^2 \frac{\partial^2 \sigma_r}{\partial r^2} + 3r \frac{\partial \sigma_r}{\partial r} + \left( 1 - \frac{E_t}{E_r} \right) \sigma_r = E_t (\alpha_r - \alpha_t) \Delta T \quad (2.16)$$

The boundary conditions are modified. The core's coefficient of thermal expansion is added to the inner boundary condition.

$$\varepsilon_t = \frac{\sigma_r}{E_c} + \alpha_c \Delta T \quad (2.17)$$

where  $\alpha_c$  is the core coefficient of thermal expansion

This yields an inner boundary condition of:



$$r \frac{\partial \delta \sigma_r}{\partial r} + \delta \sigma_r \left( 1 - \nu - \frac{E_t}{E_c} \right) = E_t (\alpha_c - \alpha_r) \Delta T \quad (2.18)$$

Using the finite difference approximations (eq. 2.11a) and solving, the boundary condition becomes:

$$\frac{r}{h} \delta \sigma_r(i+1) + \left( 1 - \frac{r}{h} - \nu - \frac{E_t}{E_c} \right) \delta \sigma_r(i) = E_t (\alpha_c - \alpha_r) \Delta T \quad (2.19)$$

The outer boundary condition assumes a traction free outer roll surface and the stress is equal to zero. Now, with these two boundary conditions (2.12)(2.19) the governing differential equation can be solved. A tri-diagonal set of simultaneous equations is produced that when solved yield incremental pressure changes due to step temperature changes. The set of equations is solved in a stepwise linear fashion. For each increment in temperature change, updated radial pressures and radial modulus are computed. Both radial pressure and modulus are pressure dependent. Quall's model steps through temperature change instead of through the roll as in Hakiel's model.

Quall's thermoelastic model was studied because his approach is the basis for the approach in this paper. Whether the core deforms due to viscoelastic behavior or thermal expansion does not alter the solution procedure. Thus, the viscoelastic model will step through time as Quall's model stepped through temperature.

### Tube Testing Device

A core testing vessel was developed by Salidis and Rowlands. [5] This vessel was used in a newly patented test method for measuring material properties tubular

samples. The method ensured that cores were tested to failure in compressive material crushing, not a structural buckling failure.

The test vessel contained an annulus of 1.5 mm. ball bearings, that were compressed radially against the outside of a core sample. The bearings were loaded by hydraulic fluid contained in a sealed bladder. The sample, bearings, and bladder were housed in a cavity within the vessel. The cavity had a hole in the bottom for venting the interior of the sample. At the top a plug was used to hold the sample in place.

This device allowed for external loading, while ensuring a uniform deformation of the core with the structure of the compressed ball bearings. Experimental stress-strain values were compared to theoretical values of aluminum tubes. Tests on aluminum tubes, with strain gages mounted on the inside of tube, showed the experimental data following the theoretical values. Paperboard tubes were tested to failure in crushing. Strain gages were placed in the hoop direction on the inside of the tube. The tests were repeated on 5 different tubes that were geometrically identical, to show repeatability.

The advantage of the test vessel Salidlis and Rowlands developed was a clean working environment. The hydraulic oil was contained in a sealed bladder. The vessel also allowed for variable size specimen with changing the size of the bearing annulus. One problem with the testing device was examining how the strain on the outer surface of the tube could be measured. The ball bearings would destroy any strain gage placed on the outside of the tube. If strain is desired on the outside of the tube another testing apparatus is needed.

## CHAPTER III

### FINDING AN EXPERIMENTAL RELAXATION FUNCTION

The creep function,  $J_c$ , is a function defining the deformation of the core over time normalized by the pressure the roll is exerting on the core. The function is found experimentally. It is an exponential function that takes the form of a generalized Maxwell equation for relaxation. [1]

$$J_c = J_0 + J_1 \exp\left(\frac{-t}{T_1}\right) + J_2 \exp\left(\frac{-t}{T_2}\right) \quad (2.6)$$

It is found by plotting the strain, normalized by pressure, versus time and fitting the curve to this equation.

An experimental apparatus was developed to simulate the wound roll stresses experienced by a core. The criteria of the apparatus is to apply stress on the outer surface of the core, while exerting no stress on the inside surface of the core. A pressure vessel was designed to exert radial pressure on the outside surface, while venting the inside of the core outside the vessel.

#### Pressure Vessel Design

The pressure vessel is designed to meet general requirements outside of this project. The pressure vessel is required to withstand a maximum pressure of 2000 psi. at room temperature. The core must be held inside the vessel. The vessel must house instrumentation or allow for leads for external instrumentation and output from internal

instrumentation. The inside of the core must be vented to atmospheric pressure to simulate an actual wound role.

The pressure vessel design selected was a round cylinder capped on both ends. This minimizes stress concentrations. A pipe was used to construct the pressure vessel, with a welded cap on one end and a flange with a blind on the other acting as a porthole. Sizing the pipe to meet the required 2000 psi. maximum pressure was accomplished using the following formula that estimates the wall thickness. [6]

$$t_m = \frac{PD}{2(SE + Py)} + A \quad (3.1)$$

Where  $t_m$  is the minimum wall thickness  
P is the maximum internal working pressure  
D is the outside diameter of the pipe  
SE is the maximum allowable stress  
y is values of joint efficiency  
A is the mechanical behavior allowance

Given a three-inch inside diameter of the core with a maximum outside diameter of four inches. The equation parameters are: [6]

P=2000 psi.  
D=6.625"  
SE=15000 lb/in<sup>2</sup>  
y=.4  
A=.065

These parameters are for a 6 inch, A106 grade B pipe.

This yields required a wall thickness of .4843 inches and a schedule 120 pipe.

The flange and cap were designed by the manufacturer for a working pressure. The flange is stamped with the maximum working pressure. A six-inch series 900 flange with a blind flange has a working pressure of 2200 psi. to 800°F. A six-inch extra heavy

welded cap has a working pressure of 2100 psi. A drawing of the pressure vessel is shown in figure 1. Pictures are shown in Appendix A figure 1 and figure 2.

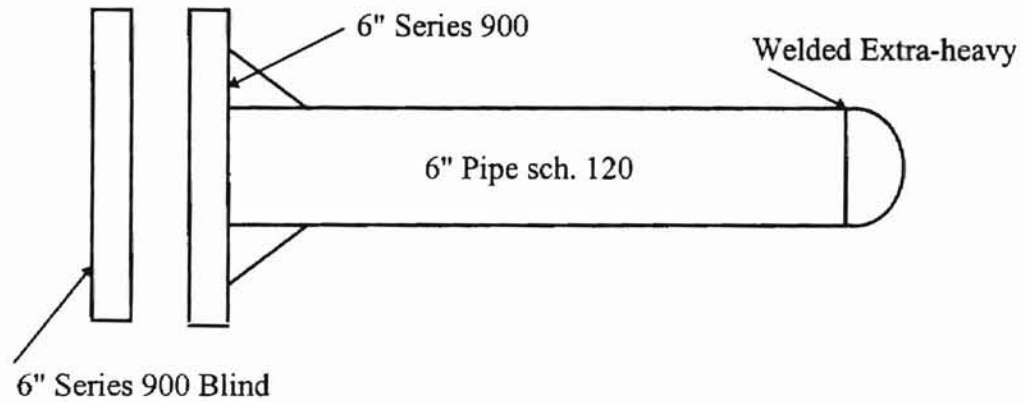


**Figure 1. Pressure Vessel**

A hollow shaft through the blind flange provides mounting for the core and venting of the inside of the core. The shaft is secured to the blind flange by a jam nut and sealed with an o-ring and washer. The core is sealed on the shaft by caps that are screwed onto the shaft and sealed with o-rings.

The pressure vessel was welded by a certified welder and met all codes and state requirements. See figure 2 for a layout of the inside of the pressure vessel.

#### Deflection Measurement

Strain was measured by a small foil patch strain gage. Two problems in using the strain gage on the paperboard core could arise because paper that makes up the core tends to absorb the glue. One, the gage is less likely to adhere to the core. Two, the glue

absorbed by the core may locally change the characteristics of the core. Both problems may give erroneous output. The glue chosen was an epoxy product from Measurements Group. It was thick enough that negligible amounts of epoxy was absorbed by the core. A picture of a gage installed upon a core is shown in Appendix A Figure 3.

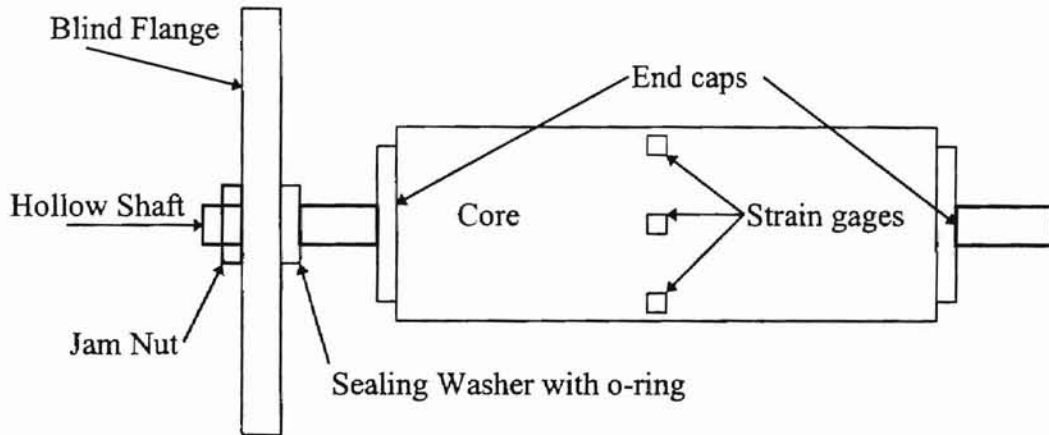


**Figure 2. Pressure vessel layout**

#### Miscellaneous Instrumentation

A bulkhead-feed through is required to route the input and output lead wires, for the strain gage, from the inside of the pressure vessel to the outside. There is a maximum of twelve wires that go through the vessel. The bulkhead-feed through consists of a wire cluster encapsulated in epoxy. This is placed directly into the blind flange.

The pressure vessel uses compressed nitrogen from bottles supplied from a local distributor. The nitrogen bottles had a capacity of 40 cubic feet at 2500 psi. To get a range of pressure inside the vessel, a Vicors pressure regulator, rated to 250 psi, was used. An analog pressure gage, mounted on the blind flange, permitted an instantaneous pressure reading.

## Data Acquisition

The strain gages, Measurements Group model CEA06-250UR-350, are placed in quarter bridge circuits with outputs resistance changes converted into strain by a Measurements Group 2103a strain indicator. The strain indicator is calibrated to read in micro-strain. The calibration equation is as follows.

$$\mu\epsilon_{\text{cal}} = \frac{R'_A}{K'(R_{\text{cal}} + R'_A)} 10^6 \quad (3.2) [7]$$

Thus, a required 10,000 microstrain resistance,  $R_{\text{cal}}$  equals 174.3 Kilo-ohms. A cantilever beam was set up to check the calibration. The theoretical strain equation is as follows:

$$\epsilon = \frac{3Dy}{L^2} \quad (3.3) [8]$$

A strain gage was mounted on a beam .5 inches wide (D), .125 inches thick (y) and 10 inches long (L). The resulting strain was calculated 1875  $\mu\epsilon$ . When the strain gage was connected to the strain indicator with the appropriate calibration factor, the strain indicator read 1876  $\mu\epsilon$ . This verified the calibration setting of the strain indicator.

An Omega PX931-KSV pressure transducer, rated at 0-1000 psi with .1% drift, was used to measure the pressure inside the vessel. This was calibrated with a dead weight tester.

An IBM clone personal computer, P-120, is used for data acquisition. LabVIEW, a graphical program for instrumentation, and an AT-MIO-16XE-50 I/O board from National Instruments, is used to store pressure and strain output.

## Experimental Procedure

Two different sets of cores of the same material with a 3-inch diameter and 0.29-inch wall thickness were provided by Sonoco. The estimated crush pressure was 400 psi and the modulus 70,000 psi. The two different sets of cores are similar in property values, but not identical. To avoid end effects, measurements were made 7 inches from the end of the core. Radial deformation is measured at the center of the length of the core. Thus, the core was cut to a length of 14 inches.

Several strain gages were mounted around the core at the center of the length, with Measurement Group M-Bond GA-2 epoxy. At times, cores do not deform in a uniform manner, thus a number of gages were used to get an average deformation.

The end caps were press fitted into the ends of the core to insure a good seal at the ends. The core was then wrapped with a 3M Poly tape to seal the outside of the core. With the paperboard cores, there was a tendency for the compressed nitrogen to seep through the core. The nitrogen would change the moisture content of the core, changing the properties. Thus, the outer tape seal was required.

After wiring the strain gages to the bulkhead feed through and connected to the strain indicator, the gages were given time to equalize. The strain indicator was zeroed and calibrated and the acquisition program was initiated. Pressure is applied to the vessel slowly and recording of the pressure and strain was made in five second intervals. This gives a core modulus of elasticity reading for each gage. After the maximum pressure for the experiment is achieved, the pressure and strain recording is changed to 120 seconds. The experiment runs for 48 hours, or until the strain has stabilized.



## Data Analysis

In order to achieve an accurate creep function over the pressure range of the core, three different pressures were tested, 100 psi, 150 psi, 200 psi. In preliminary examination of the testing procedure, it was found that testing at above 50% of crush pressure, a buckling phenomenon may have occurred. Thus, the maximum 200 psi test pressure is 50% of the 400 psi crush pressure rating of the cores.

Pressure, time, and strain from all gages were recorded at each of the given pressures. The pressure and strain data taken during the initial start up, through the elastic range, was used to calculate the elastic modulus. An elastic modulus of 80,000 psi,  $\pm 10,000$  psi reading on each strain gage, was used as an assessment of the accuracy of the gage reading. If the elastic modulus was not within the 80,000 psi  $\pm 10,000$  psi range it was removed from the analysis. The most likely cause of faulty gauge data is improper attachment of the gauge or a flaw in the core.

Core analysis from the first set of cores are shown first. The data for the second set of cores will be analyzed in the same manner, following the first set. The plots in Figure 3 show the strain data at the three set pressures for the first set of cores.

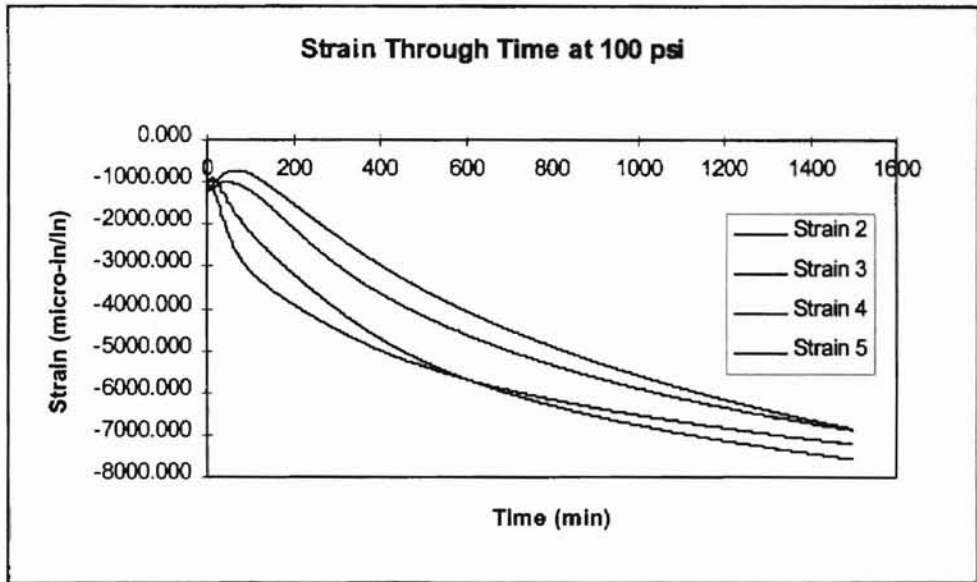


Figure 3a. Strain Data for Core #1 at 100 psi.

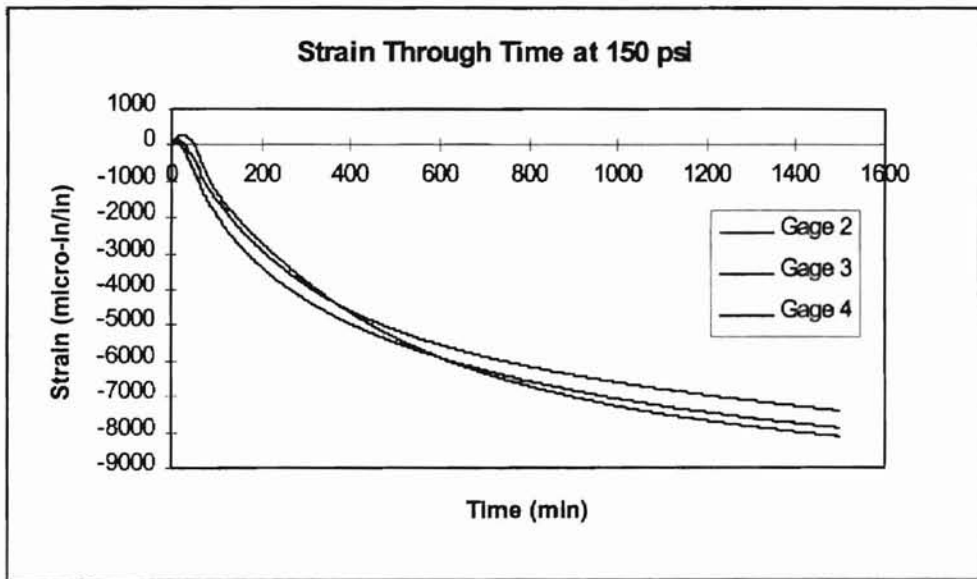


Figure 3b. Strain Data for Core #1 at 150 psi.

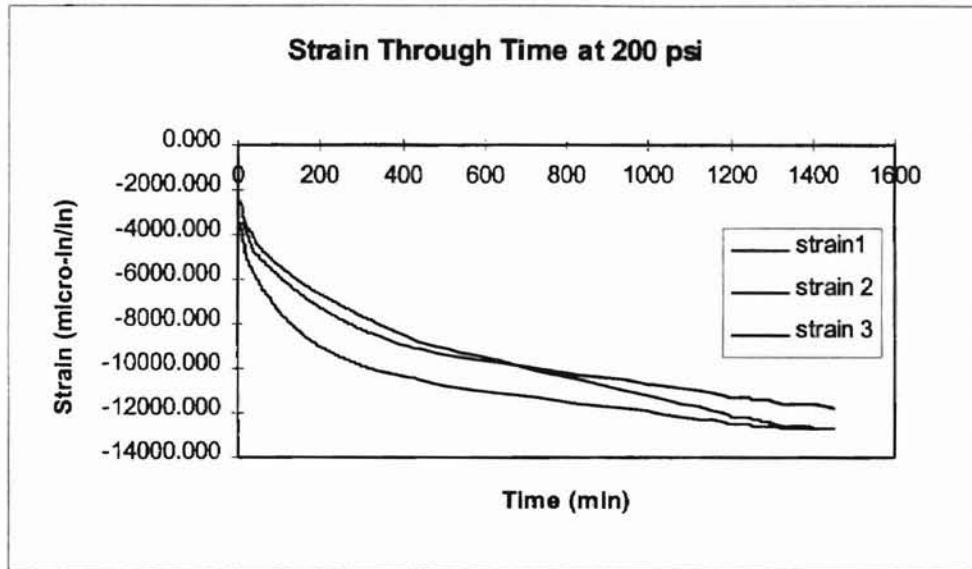


Figure 3c. Strain Data for Core #1 at 200 psi.

The plots in figure 3 show a variation in strain between individual gages within a given pressure. This is due to the core not deforming uniformly because of inconsistency within the core. Therefore, the strain from each gauge is averaged to get an average deformation across the entire core. The elastic strain was then subtracted in order to isolate the strain caused by creep. Figure 4 shows the average strain.

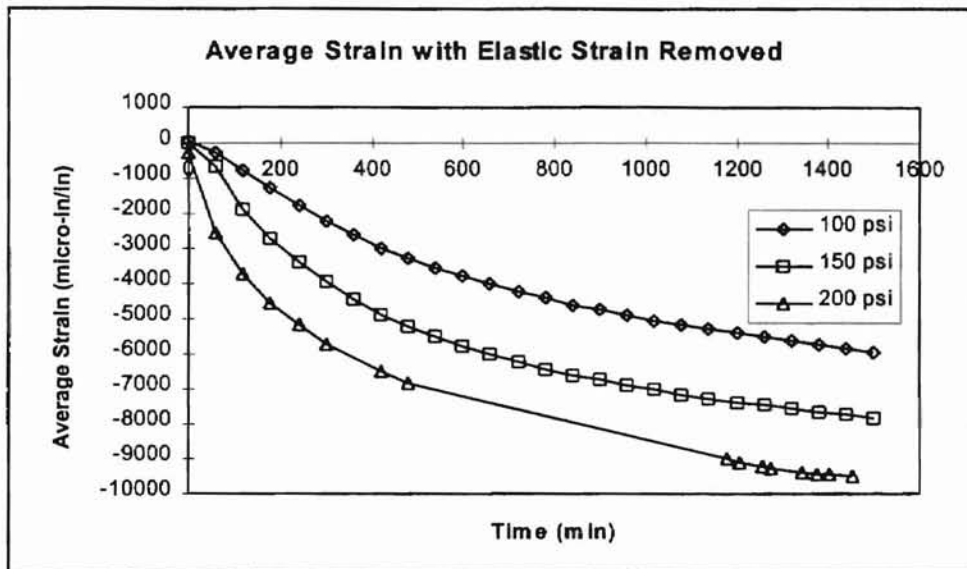


Figure 4. Average Strain Data for Core #1

The family of curves produced by these tests do not follow the same path. A function was needed to associate the curves so that they may be modeled as a Maxwell model. Normalizing the strain curves, by dividing by their associate pressures, the normalized curves can be fit with the Maxwell model. This is shown in figure 5.

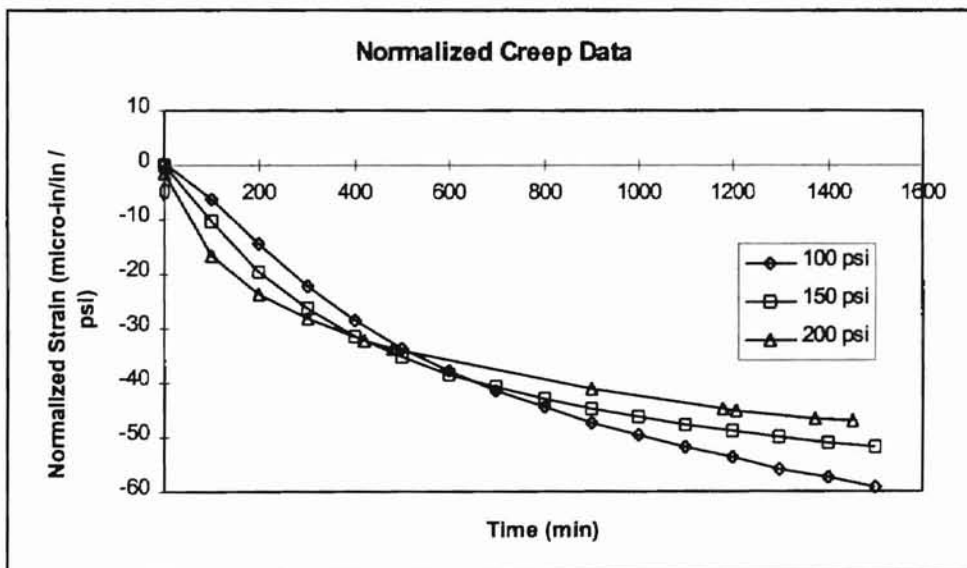


Figure 5. Normalized Creep Plot for Core #1

The lines of normalized strain, the strain divided by the corresponding pressure, follow similar paths. They were represented by a single creep function, derived from the generalized Maxwell creep function discussed earlier. The normalized strain is averaged and a creep function is estimated. The error introduced into the analysis by averaging the normalized strain and developing a creep function was insignificant, due to the magnitude of the strains and the size of the deviation of the normalized strains. This is reinforced in the testing results in Chapter V. The coefficients to the creep function were found by utilizing an EXCEL worksheet solver function. Within the worksheet, the creep function is compared to the data at each time point. The difference is then summed and minimized by changing the function coefficients, thus getting an appropriate creep function. The EXCEL Solver function yields the following equation.

$$J = -60.06 + 17.82e^{\frac{-\text{time}}{221.31}} + 42.24e^{\frac{-\text{time}}{865.50}} \quad (\text{micro-in/in / psi}) \quad (3.4)$$

A plot of the creep function versus the normalized creep data is shown in Figure 6.

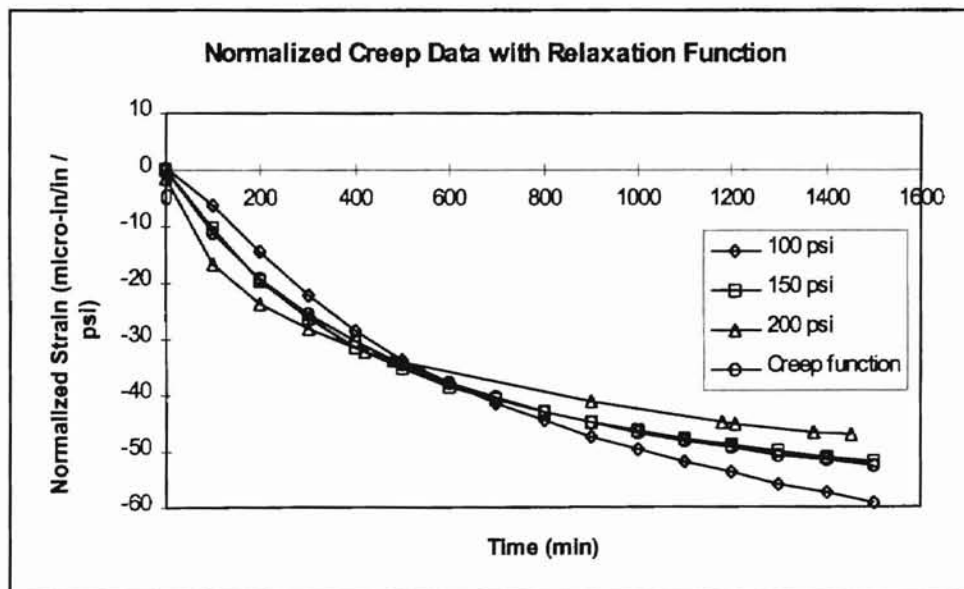


Figure 6. Creep Function Plot of Core #1

The Maxwell Model follows the average strain data. The average normalized creep data seems to be diverging as time progresses past the time shown. Thus, the Maxwell creep function is only applicable through this time period.

The analysis on the second set of core data follows in the same manner as the first set. The strain data for the second set of cores are seen in Figure 7.

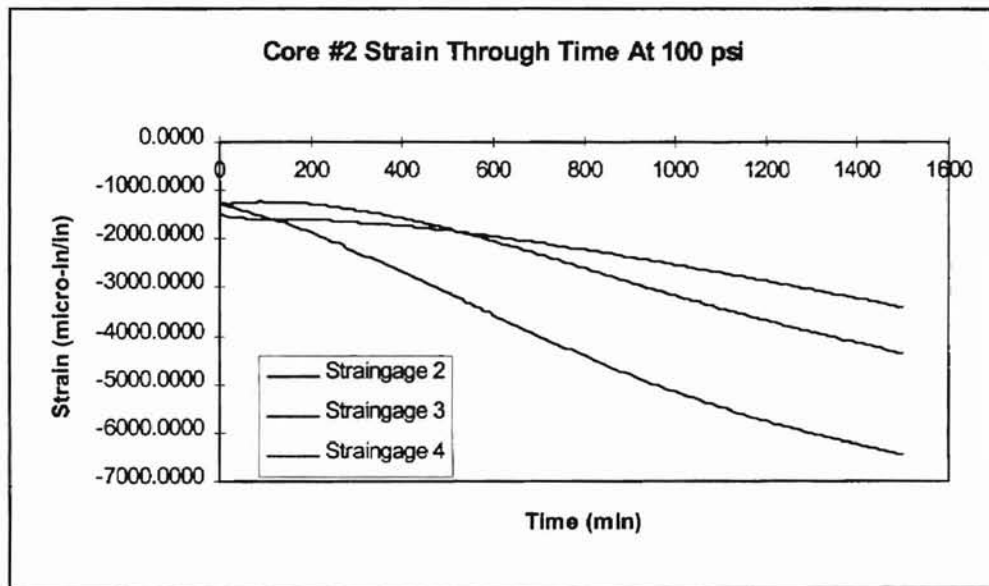


Figure 7a. Strain Data for Core #2 at 100 psi.

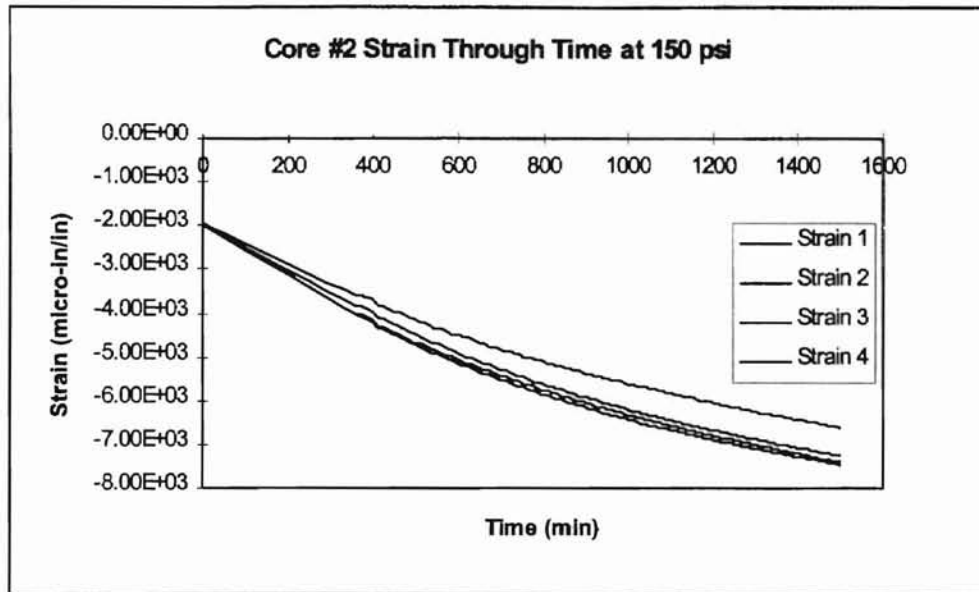


Figure 7b. Strain Data for Core #2 at 150 psi.

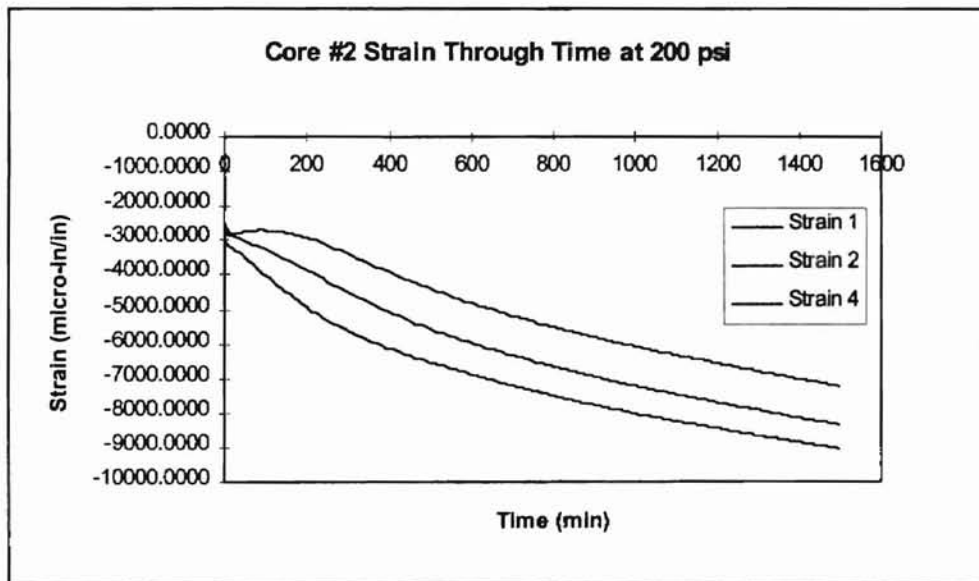


Figure 7c. Strain Data for Core #2 at 200 psi.

The strain data is averaged with respect to its pressure and shown in Figure 8.

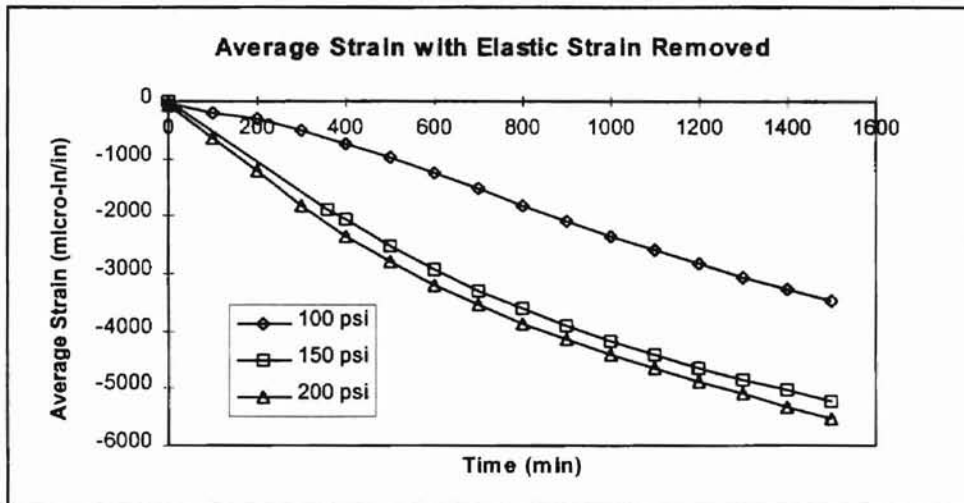


Figure 8. Average Strain Data for Core #2

The average strain is normalized by dividing by the test pressure and is shown in

Figure 9.

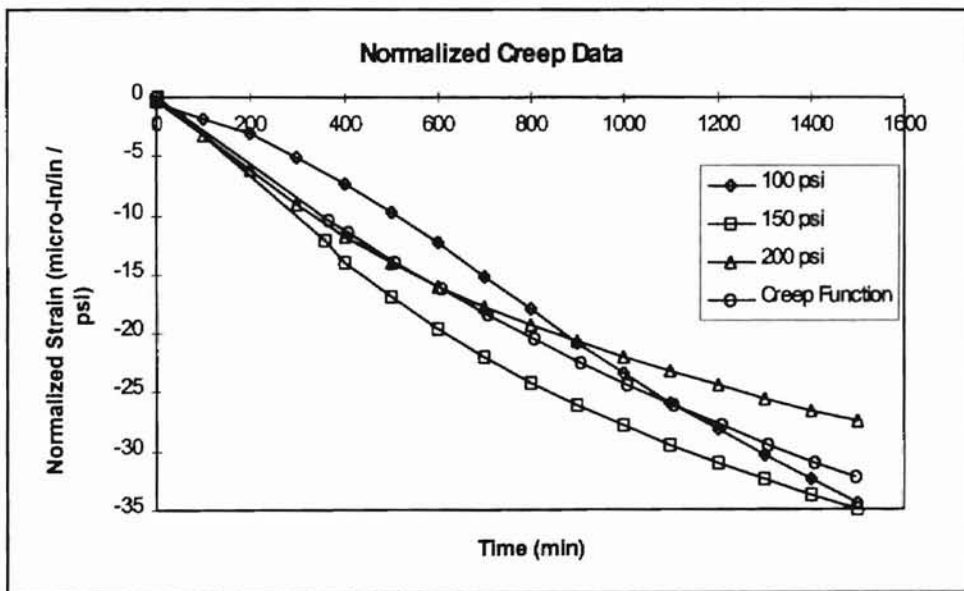


Figure 9. Normalized Creep Plot for Core #2



Using the EXCEL equation solver in the same manner as for core #1 with the average of the normalized creep data, the general Maxwell creep function is obtained.

The equation is :

$$J = -5.96 + 0.0892 * e^{\frac{-\text{time}}{122.86}} + 59.51 * e^{\frac{-\text{time}}{1917.88}} \quad (\text{micro-in/in / psi}) \quad (3.5)$$

A plot of the creep function verses the normalized creep data is shown in Figure

10.

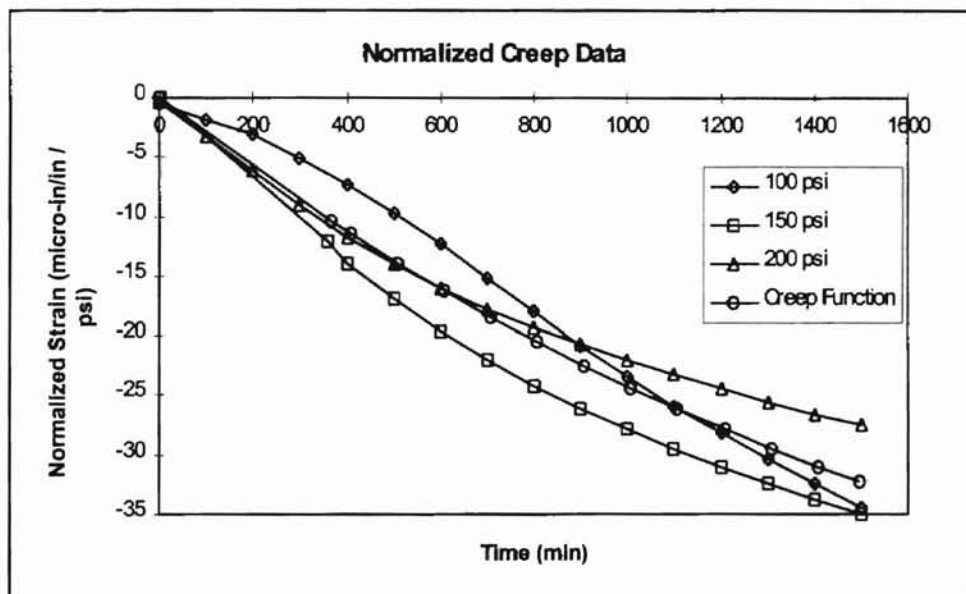


Figure 10. Creep Function Plot of Core #2

The Maxwell creep function fits the average normalized data. However, the normalized average data diverge as the time continues. This function is only representative of the normalized data at shorter time intervals.

In a roll, the core will experience a pressure change as the core deforms. All of these tests are executed at constant pressures. But, with the Maxwell creep function modeled through a pressure range, a pressure may be calculated given the deformation at a given pressure within the range. A mathematical model will be developed to accomplish this job.

## CHAPTER IV

### ROLL MODEL

The core is influenced by pressure due to the wound roll above it. This pressure does not remain constant. As the core deforms under the pressure of the roll through time, the roll pressure decreases. Thus, a model is needed to predict the deformation of the core and the resulting pressure change through time.

The model begins with a wound roll on a core. The initial pressures within the wound roll are found by using Hakiel's Model, discussed in Chapter II. The time varying model is developed just as Hakiel's Model. Hakiel's model applies to the wound roll in that the governing differential equation (2.12) does not change. [3]

$$r^2 \frac{\partial^2 \sigma_r}{\partial r^2} + 3r \frac{\partial \sigma_r}{\partial r} + \left(1 - \frac{E_t}{E_r}\right) \sigma_r = 0 \quad (2.12)$$

and with the central difference approximations included the equation (2.18) is:

$$\left(\frac{r^2}{h^2} - \frac{3r}{2h}\right) \sigma_r(i-1) + \left(\frac{-2r^2}{h^2} + 1 - \frac{E_t}{E_r}\right) \sigma_r(i) + \left(\frac{r^2}{h^2} + \frac{3r}{2h}\right) \sigma_r(i+1) = 0 \quad (2.18)$$

The boundary conditions are where this model and Hakiel's Model differ. The boundary condition at the core-roll interface is calculated by assuming the deflection of the core is equal to the deflection of the first layer of the roll.

$$\mathbf{u}_{mat'l} = \mathbf{u}_{core} \quad (4.1)$$

divide both sides by radius of the core

$$\varepsilon_{\text{mat'l}} = \varepsilon_{\text{core}} \quad (4.2)$$

First, we will focus upon the strain in the web material. Starting with the equilibrium equation (2.7) and substituting it into the constitutive equation (2.8b) yields:

$$\varepsilon_{t,\text{matl}} = \frac{1}{E_t} \left( r \frac{\partial \sigma_r}{\partial r} + \sigma_r \right) - \left( \frac{v_{tr}}{E_r} \right) \sigma_r \quad (4.3)$$

Applying the central difference approximations for first derivative,

$$\frac{\partial \sigma_r}{\partial r} = \frac{\sigma_{rj}(i+1) - \sigma_{rj}(i)}{h} \quad (2.17a)$$

where  $j$  denotes the stress at the current point in time yields:

$$\varepsilon_{\theta\theta,\text{matl}} = \frac{1}{E_t} \left[ r \left( \frac{\sigma_{rj}(i+1) - \sigma_{rj}(i)}{h} \right) + \sigma_{rj}(i) \right] - \frac{v_{tr}}{E_r} \sigma_{rj}(i) \quad (4.4)$$

rearranging, we have:

$$\varepsilon_{\theta\theta,\text{matl}} = \left( \frac{r}{h} \frac{1}{E_t} \right) \sigma_{rj}(i+1) + \left( \frac{1}{E_t} - \frac{r}{h} \frac{1}{E_t} - \frac{v_{tr}}{E_r} \right) \sigma_{rj}(i) \quad (4.5)$$

Since roll winding is an accretive process and the pressures which are computed affect the radial modulus,  $E_r$ , the second order differential equation in radial pressure is solved several times for differences in pressure which are summed to yield total pressures in each layer. So the previous expression is typically cast in the form:

$$\varepsilon_{\theta\theta,\text{matl}} = \left( \frac{r}{h} \frac{1}{E_t} \right) \delta\sigma_{r,j}(i+1) + \left( \frac{1}{E_t} - \frac{r}{h} \frac{1}{E_t} - \frac{v_{tr}}{E_r} \right) \delta\sigma_{r,j}(i) \quad (4.6)$$

Now, let us focus upon the strain in the core. The strain at the core is defined as:

$$\epsilon_{\text{core}} = \int J_c(t-t') \frac{d\sigma_r}{dt} dt' \quad (4.7) \text{ (Ref. 9)}$$

The integral will be approximated at each step in time as:

$$\epsilon_{\text{core},\Delta t} = J_c(t_j - t_{j-1}) \sigma_{r,j-1}(i) \quad (4.8)$$

To obtain the total core strain at any point in time, the strains at each time step must be summed as:

$$\epsilon_{\text{core,total}} = \sum_{n=1}^{n=j} J_c(t_j - t_{n-1}) \sigma_m(i) \quad (4.9)$$

Equation (4.9) yields the viscoelastic strain at a given time increment. Elastic strain of the core (4.10) must also be added to the equation.

$$\epsilon_{\text{core,elastic}} = -\frac{\sigma_{r,j}(i)}{E_c} \quad (4.10)$$

Now, assuming the generalized Maxwell form for the relaxation function from equation (2.6) yields:

$$\epsilon_{\text{core},\Delta t} = \left( J_0 + \sum_{i=1}^2 J_i e^{\frac{-\Delta t}{T_i}} \right) \sigma_{r,j-1}(i) \quad (4.11)$$

Now, equating the strain in the core and in the web material yields:

$$\left( \frac{r}{h} \right) \delta \sigma_{r,j}(i+1) + \left( 1 - \frac{r}{h} - \frac{E_t}{E_c} \right) \delta \sigma_{r,j}(i) - \left( J_0 + \sum_{i=1}^2 J_i e^{\frac{-\Delta t}{T_i}} \right) \sigma_{r,j-1}(i) = 0 \quad (4.12)$$

The outer boundary condition is calculated assuming a traction free outer roll surface.

$$\sigma_r(r = r_{\text{out}}) = 0 \quad (4.13)$$

With these two boundary conditions, the governing differential equation can be solved for the static, time dependent region of the model.

With the boundary conditions (4.12), (4.13), the governing differential equation can be solved. The set of tri-diagonal simultaneous equations are set up and solved in the same manner as the Quall's model described in Chapter II, with the exception of stepping through time instead of through temperature. The set of equations are solved in a stepwise linear fashion through time that yields increments in pressure decay. Then, the radial pressures and radial modulus are updated each time step. The final solution yields a pressure profile of the roll through time.

### Computer Model

The finite difference method of solving differential equations can be readily solved on a personal computer. A FORTRAN code was developed to solve the model and output the solution. The algorithm flow chart is shown in figure 11. A listing of the FORTRAN code is in Appendix B.

The program requires the user to input some system requirements and material properties. The system requirements are: winding tension, outside radius of the core, outside radius of the roll, number of increments through the roll, total time, and number

of increments through time. The material properties required are: radial stiffness and Poisson's ratio of the core, the third order polynomial for the radial modulus of the web, tangential modulus of the web, and the directional Poisson's ratio's of the roll.

The program outputs five columns of radial position, radial stress, and incremental stress change. The output format lends itself to its use in a spreadsheet software, such as Microsoft EXCEL. In EXCEL, one can plot the radial stress versus time.

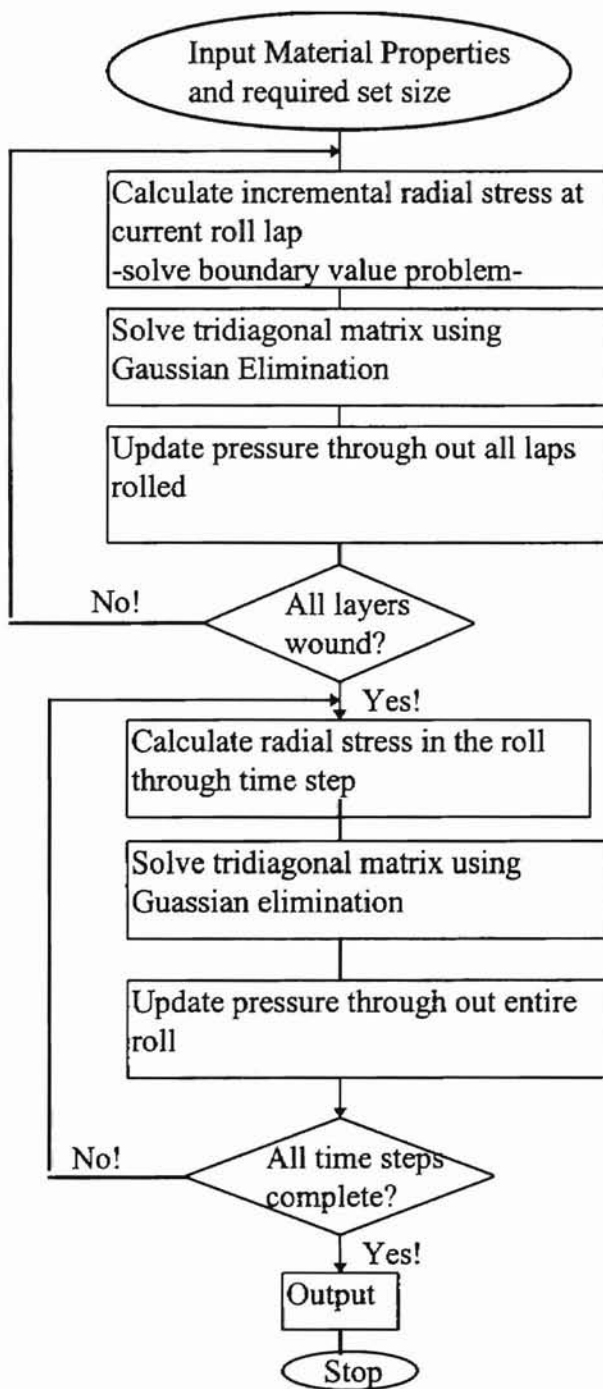


Figure 11. Flow chart.



## CHAPTER V

### MODEL VERIFICATION

The roll model calculates the radial stresses due to the combination of the winding of the roll and the deformation of the core through time. It begins at time zero and ends at a specified time. The model was developed previously in this paper. The FORTRAN code was used with the given core properties and the properties of a polyester film. The properties are as follows.

Roll ID = 1.75 in  
Roll OD = 5.75 in  
Roll Iterations = 1000  
Winding Tension = 2000 psi  
ICI "377" 200 gauge film  
     $E_r = 54.97 * P - .07819 * P^2 + .0001388 * P^3$  (psi)  
     $E_t = 600000$  (psi)  
Core E = 80000 (psi)  
Creep Coefficients (micro-in/in / psi)  
     $J_0 = -60.059$   
     $J_1 = 17.817$   
     $T_1 = 221.31$   
     $J_2 = 42.242$   
     $T_2 = 865.50$

The film  $E_r$  property equation comes from a stack test. A stack of loose web was compressed with the normal pressure and strain recorded. The slope of this data was used to generate this  $E_r$  third order polynomial as a function of pressure. The film  $E_t$  property is established in a tensile in-plane stress verses strain test.

The roll pressure builds very quickly during winding. Figures 12 and 13 show how the radial pressure develops in the roll and how the pressure varies during winding,

respectively. Note, the core pressure has nearly reached its maximum value after eleven minutes from a total winding time of 70 minutes.

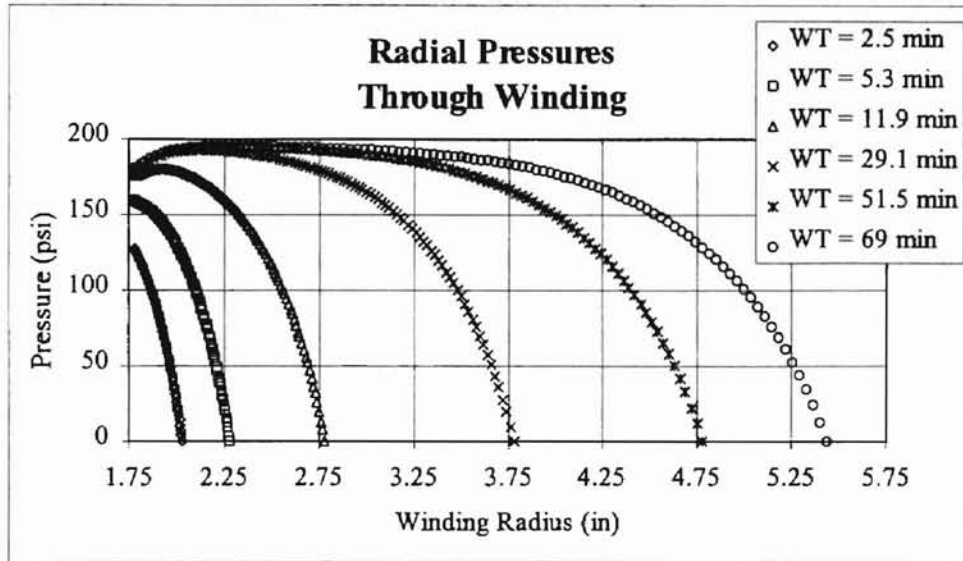


Figure 12 Radial Pressure Through Winding

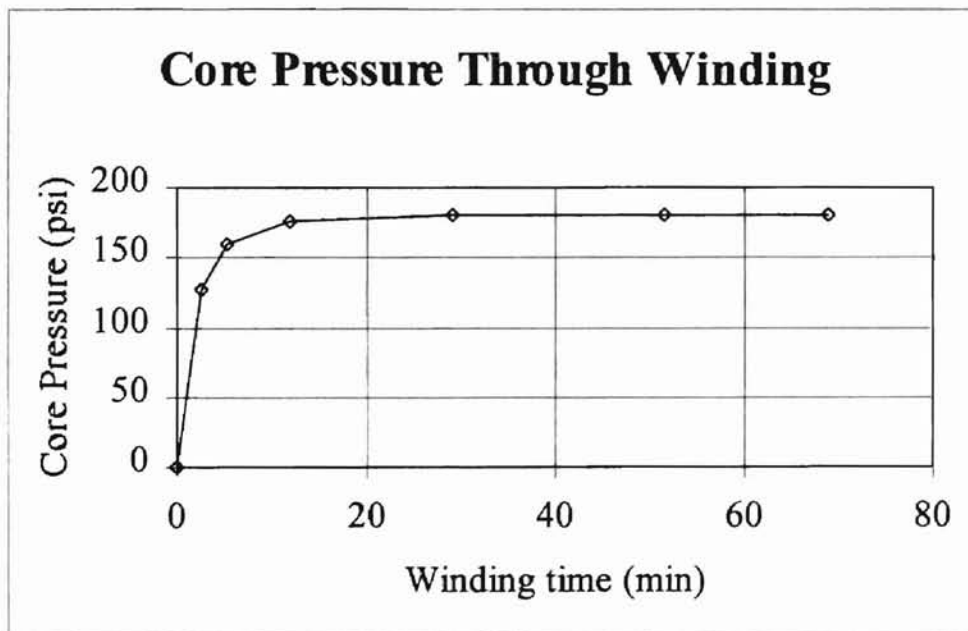


Figure 13. Core Pressure Through Winding

## Roll Testing

Six wound rolls of ICI 377-200 film were made in accordance with the previous parameters. The first three rolls were tested by instrumenting the core with strain gauges and measuring the core strain over time. The results were found to be widely varying. This was caused by the way the strain was read. The gauges were mounted on the core and connected to the strain indicators. The gauges were unable to be connected to the indicator during winding of the roll, so they were disconnected. After winding, the gauges were reconnected. Connection of the gauges consisted of twisting wires together which, if connection changes occur, can change the resistance of the lead wires. The theoretical resistance change within the system using the gauge factor, was 1 to 2 ohms. This was seen in leadwire resistance change in connections alone. Thus, this method of testing was inconclusive and a new method had to be developed.

Note, this problem had no impact on the pressure chamber testing. The connections were not disconnected during the test and the leadwire resistance did not change. Instrumentation was zeroed before testing began, thus taking the lead wire resistance into account.

A new test method was derived from the same method used by Hakiel in his study of wound roll stresses. [3] The interlayer pressures were calculated by forcing two layers of the web, close to the core, to slip upon one another. The layers of web to be tested are not in direct contact with the core. If these layers were to be used, problems may arise. The friction coefficient between the core and web is not known and difficult to calculate. Sliding the web from a compressed core section over an uncompressed section would

lead to problems with binding. Finally, shearing of the tape bonding of the web to the core, required at the start of the winding process, would require an unknown force. In order to eliminate these problems, layers of web removed from the core are used in the test.

By knowing the web to web static coefficient of friction, and reading the force required to slide the web, the interlayer pressure can be found.

$$F = \mu_k N \quad (5.1)$$

The interlayer pressure (P) is found by the interlayer force divided by the surface area.

$$P = \frac{N}{2\pi r w} \quad (5.2)$$

The force required, to cause the web layers to slip, was provided by a material testing system, INSTRON model 8502. Figure 15 shows the test setup. Dies were created to ensure the repeatability of the correct web layers sliding on each test. The bottom male die has a running fit to the outside diameter of the core. It has an outside diameter of 1.95". The top female die has a loose fit to the outside diameter of the male die. This is so that the web will be pushed up by the male die into the bottom die and so that the correct web layers slide in each of the tests performed. Figure 14 shows the die set.

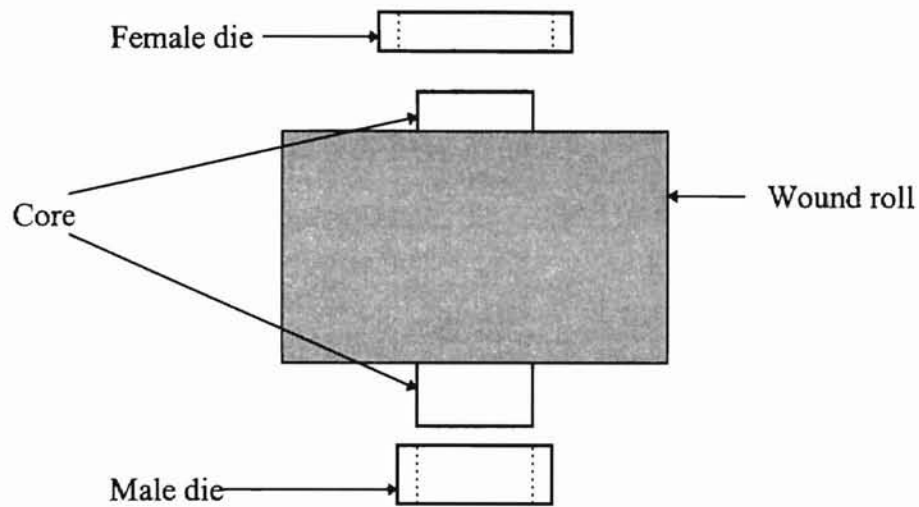


Figure 14. Die Set

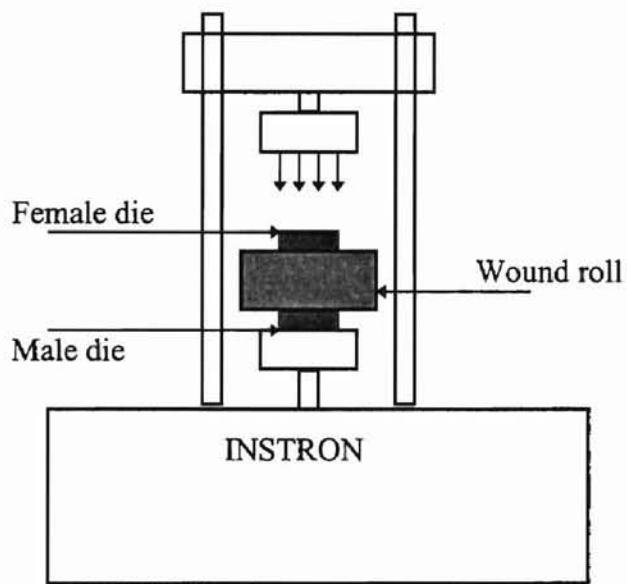


Figure 15. Push Test Set Up

Each roll is tested over a 1500 minute time interval. The roll was placed in the INSTRON press with the two dies placed as in previous figure. The INSTRON press was set to move 0.01" per second. The force was recorded along with the displacement.

When the required web layer begins to slip past each other, the pressure levels off. This

was the push force required. The force and displacement were recorded on a PC and the slip pressure was read from the record.

## RESULTS

Rolls #1, #2, and #3 were tested under the strain acquisition procedure in which data received was deemed unusable.

Roll #1  
Core type #1  
Web: ICI-377-200 gauge  
Coefficient of Friction: .21  
OD: 11.5"  
ID: 3.5625"  
Winding Tension: 1700 psi  
Winding Speed: 50 ft/min

Note, the coefficient of static friction was found by employing tests on web material in the same fashion as described by Ducotey. [10]

Roll #2  
Core type #1  
Web: ICI-377-200 gauge  
Coefficient of Friction: .21  
OD: 11.625"  
ID: 3.5625"  
Winding Tension: 2000 psi  
Winding Speed: 50 ft/min

Roll #3  
Core type #1  
Web: ICI-377-200 gauge  
Coefficient of Friction: .21  
OD: 10.625"  
ID: 3.5625"  
Winding Tension: 2000 psi  
Winding Speed: 50 ft/min

Pictures of Roll #2 and Roll #3 are in Appendix A, figure 4 and figure 5, respectively.

Roll #4 was the first roll to undergo this push test through a step time interval.

The winding parameters are the same as in the model with the exception of the following:

Roll #4  
Core type #1  
Web: ICI-377-200 gauge  
Coefficient of Friction: .21  
OD: 10.875"  
ID: 3.5625"  
Winding Tension: 2000 psi  
Winding Speed: 50 ft/min

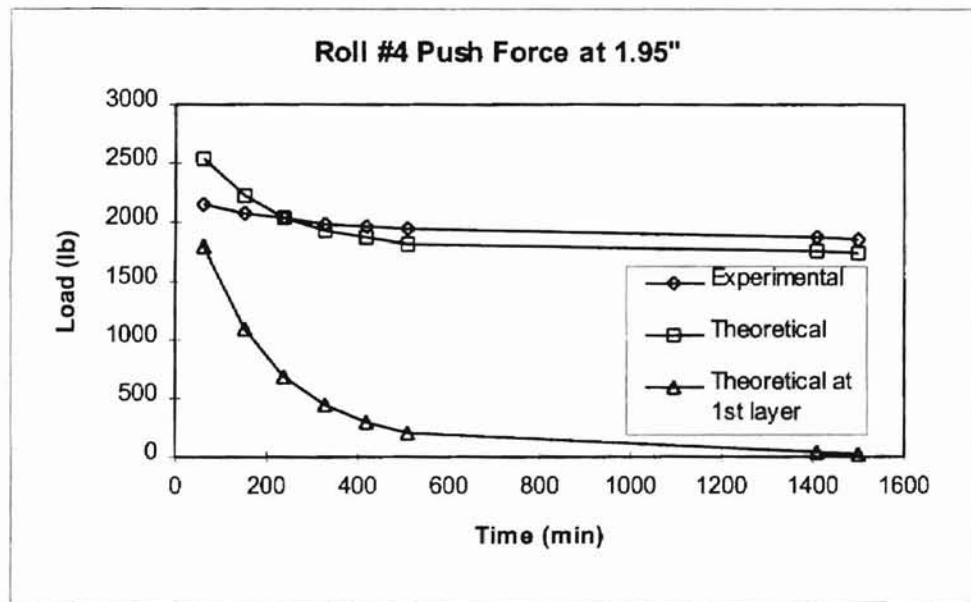


Figure 16. Roll #4 Push Force

In figure 16, the experimental push force is plotted along with the values predicted from the computer model. Also, the plot displays the predicted force to push the first two layers by one another. This shows the drop in pressure at one layer past the core and an indication of the core pressure.

The Roll #4 push force data through time follow the model well. At the first few time intervals, however, the data diverge. This may be due to the layout of the roll and the core type. The outside of the roll is rough and sticks out of the roll several inches. During the first few tests, the die did not slide smoothly due to the snug fit of the die against the core. After the sides of the core had worn a little, the data seem to correlate better.

Notice that after 1500 minutes, the pressure near the core drops to zero. Then the core will no longer deform viscoelastically. A plot of the radial pressure of the roll at time = 0 and time = 1500 minutes is shown in figure 17.

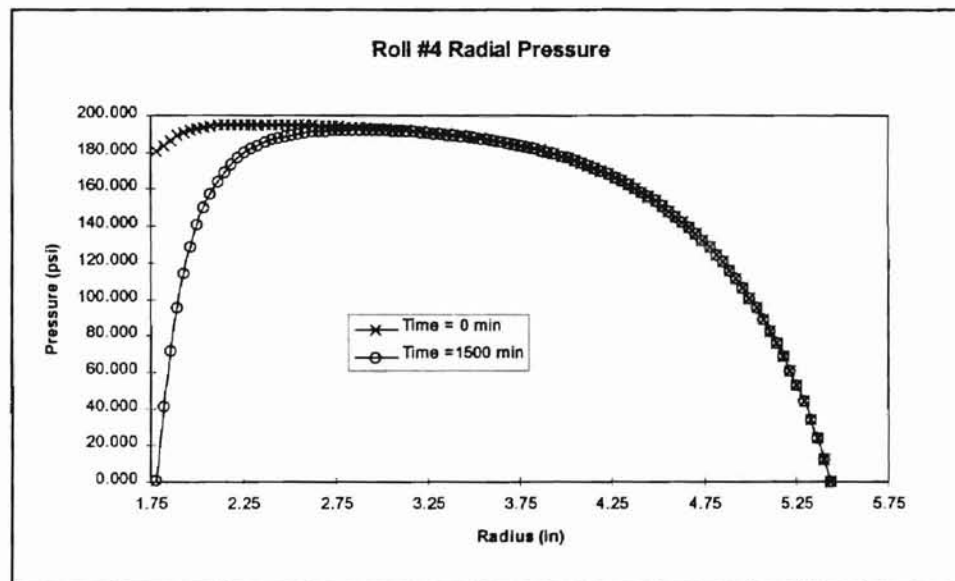


Figure 17. Roll #4 Radial Pressure

The figure shows that the model is accurately predicting the later time intervals and need not be estimated further.

Roll #4 developed a starring flaw at the core roll interface during the winding, due to the deformation of the core and the pressure change of the roll. This flaw is shown in a picture in the Appendix A figure 6.



Roll #5 was the next roll to undergo this push test. The winding parameters are the same as in the model with the exception of the following:

Roll #5  
Core type #2  
Web: ICI-377-200 gauge  
Coefficient of Friction: .21  
OD: 11.75"  
ID: 3.5625"  
Winding Tension: 2000 psi  
Winding Speed: 50 ft/min

A picture of roll #5 is found in Appendix A figure 7.

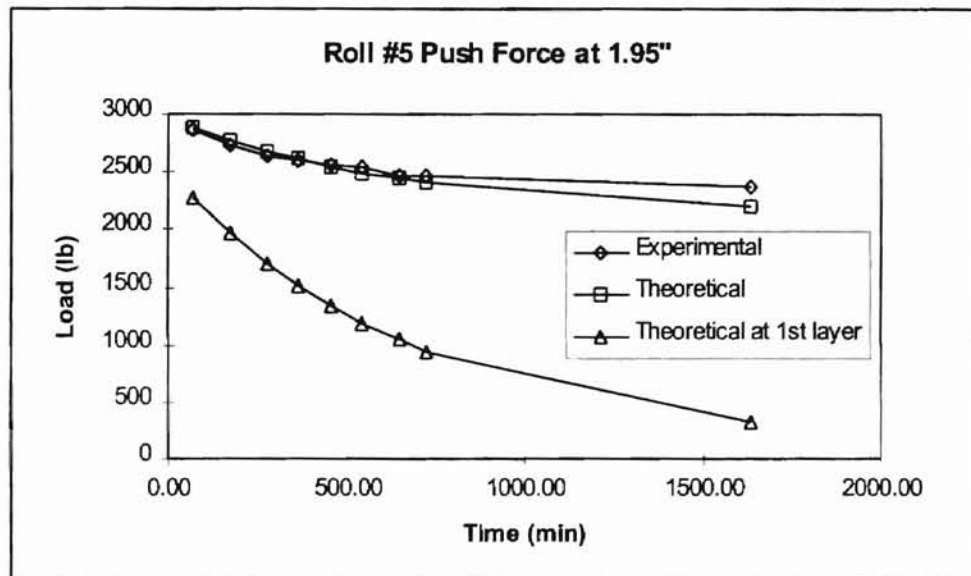


Figure 18. Roll #5 Push Force.

This plot is set up the same as the previous plot for Roll #4. They are similar. Roll #5 correlates better at first. The core type #2 is smooth and stuck out of the roll by only a half an inch. The data seem to diverge at the end of the test period. This is due to the model creep function which did not fit the normalized averages of the core data at the longer time periods. A plot of Roll #5 radial pressure through time is shown in figure 19.

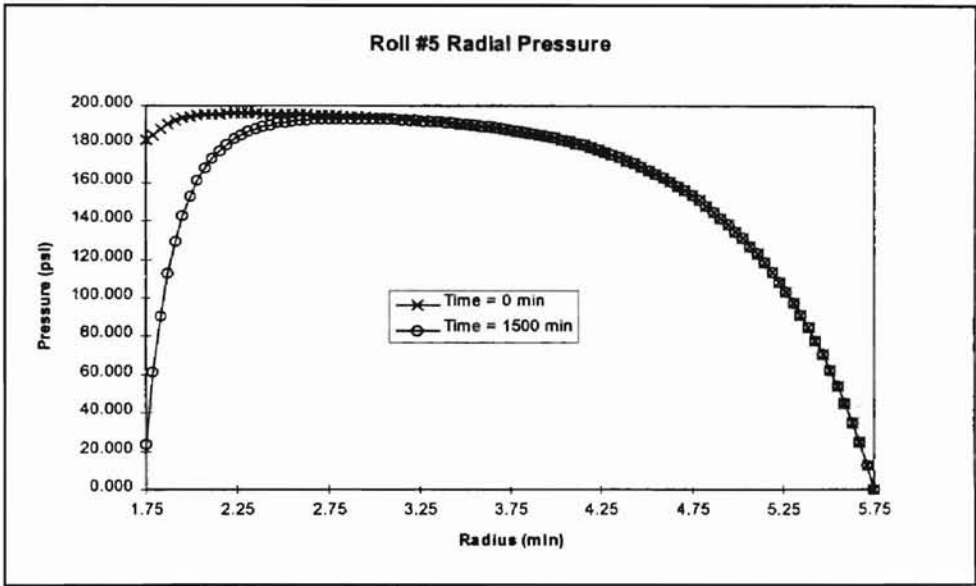


Figure 19. Roll #5 Radial Pressure.

## CHAPTER VI

### CONCLUSIONS

This study has shown how the viscoelastic properties of the core effect a wound roll. The viscoelastic core properties are represented by a relaxation function. The relaxation function is found experimentally by submitting cores to a series of constant stress tests over time. The strain is recorded and normalized by dividing by the test pressure. A relaxation function is fitted to the average of the normalized strain. The function can then be used in the developed mathematical model to predict wound roll behavior. Model verification tests show that the model can accurately predict the stresses through the roll.

Viscoelasticity of the core will cause the core pressure to decrease over time and finally decay to zero. This is a localized phenomenon and does not affect the entire roll. The pressure decay at the core is, however, significant. It can cause staring to occur, as seen in a picture in Appendix A figure 6.

The verification tests show that an accurate creep function is needed. In core type 2, the creep function does not accurately predict the strain data at the later test times. This caused a divergence in the accuracy of the model.

This model is a tangible way to predict the pressure decay within a wound roll in the vicinity of the core. The web handling industry will find this research useful.

## CHAPTER VII

### FUTURE WORK

This model was developed with the assumption that viscoelastic properties of the core were not affected during the winding of a roll. A new model can be developed to include the creep function during the winding process. There will be situations where the pressure would drop appreciably during winding.

This study was conducted under conditions in which temperature and humidity were held constant. In industry, wound rolls are submitted to environmental changes which may affect the core. The environmental conditions need to be considered.

The two cores shown in this study were similar but not the same. Their relaxation functions were different. A correlation can be developed to relate different core types.

## REFERENCES

1. Findley, William N., Lai, James S., and Onaran, Kasif, Creep and Relaxation of Nonlinear Viscoelastic Materials, North Holland Publishing Company, New York, 1976.
2. Gerhardt, T.D., "External Pressure Loading of Spiral Paper Tubes: Theory and Experiment". Sonoco Products Company, Madison, WI.
3. Hakiel, Z., "Nonlinear Model for Wound Roll Stresses", Tappi Journal, May 1987. Pg. 113-117.
4. Qualls, William R. & Good, J. Keith, "Thermal Analysis of a Wound Roll", Accepted by Journal of Applied Mechanics, January 1997.
5. Salikis, Edmond P. & Rowlands, Robert E., "A Novel Radial Compression Testing Device for Tubes", Tappi Journal, January 1997. Pg. 234-237.
6. ASME B31.3-1996 Edition, Process Piping, ASME Code for Pressure Piping, B31 an American National Standard, The American Society of Mechanical Engineers, 1996. Pg. 304.1.1-304.1.2, Table A-1, A-1A.
7. Measurements Group, "Strain Gage Conditioner and Amplifier System Instruction Manual", Raleigh, North Carolina, 1992.
8. Shigley, Joseph E., & Mischke, Charles R., Mechanical Engineering Design, 5th ed., McGraw-Hill, New York, 1989.
9. Qualls, William R., Hygrothermomechanical Characterization of Viscoelastic Centerwound Rolls, Ph.D. Dissertation, Oklahoma State University, May 1995.
10. Ducotey, Keith S. Traction Between Webs and Rollers in Web Handling Applications, Ph.D. Dissertation, Oklahoma State University, May 1993.

APPENDIX A

PICTURES



Figure A-1, Fixture Set-up #1.

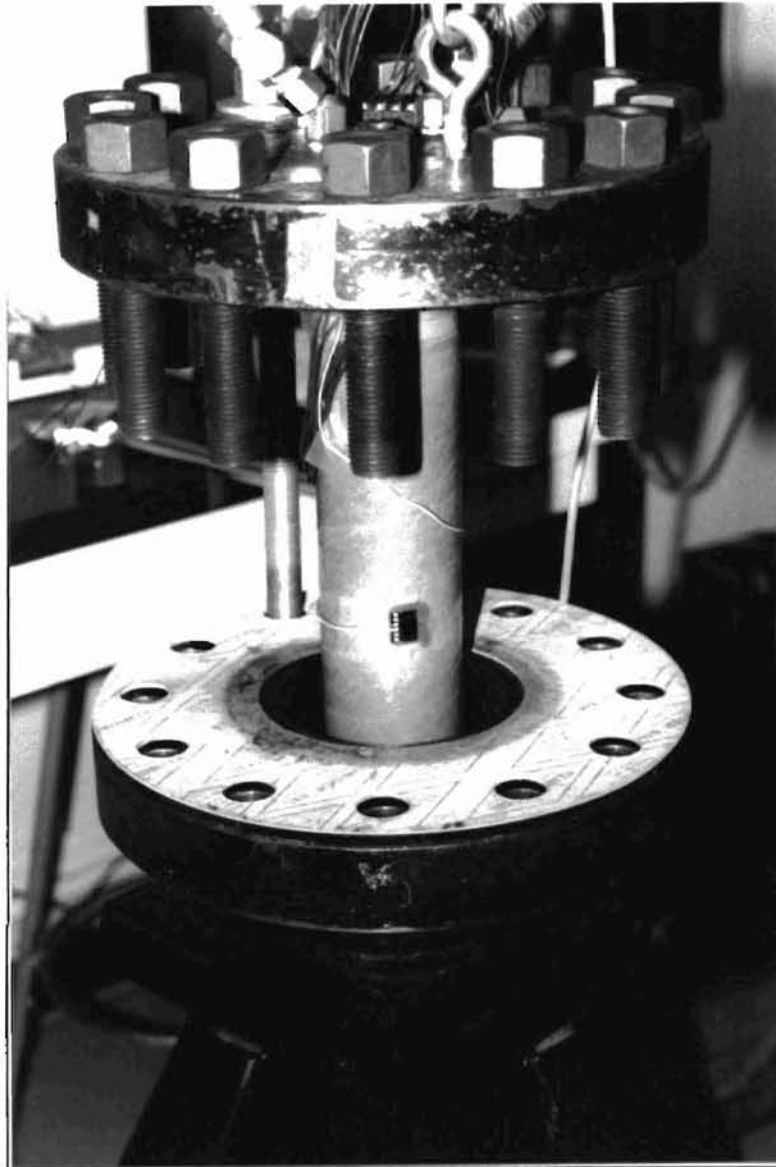


Figure A-2, Fixture Set-up #2.



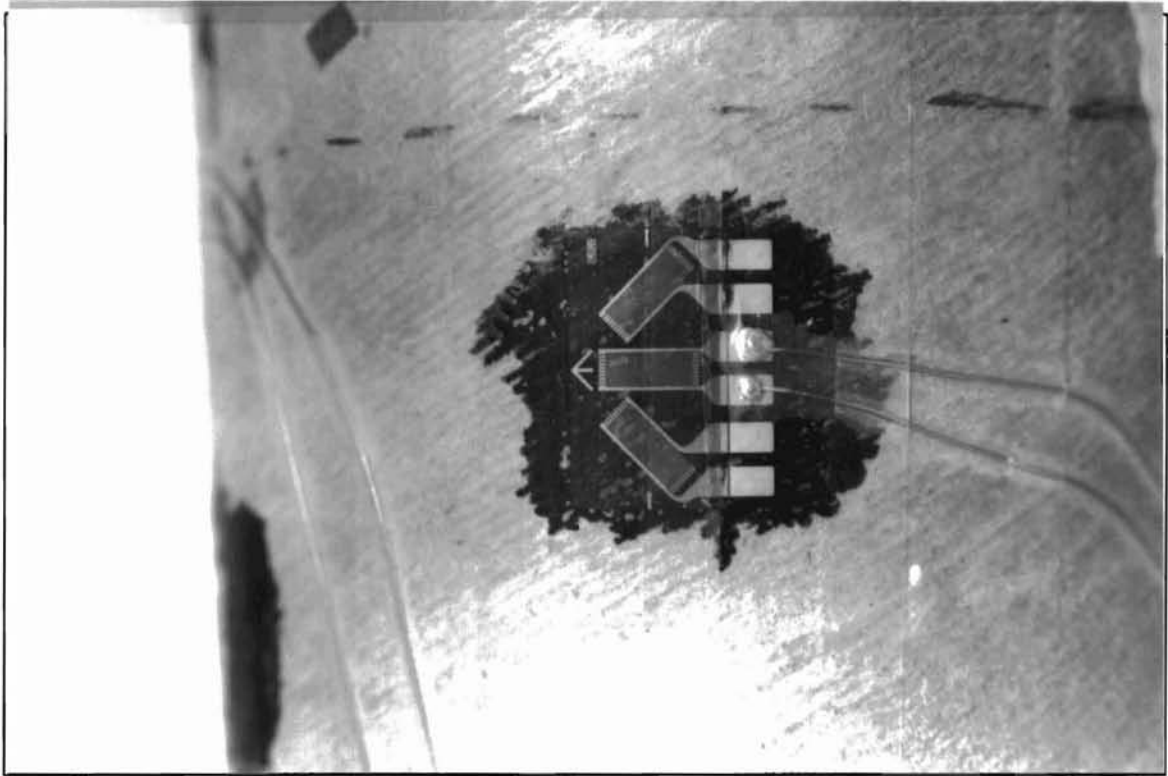


Figure A-3, Strain Gage Application.

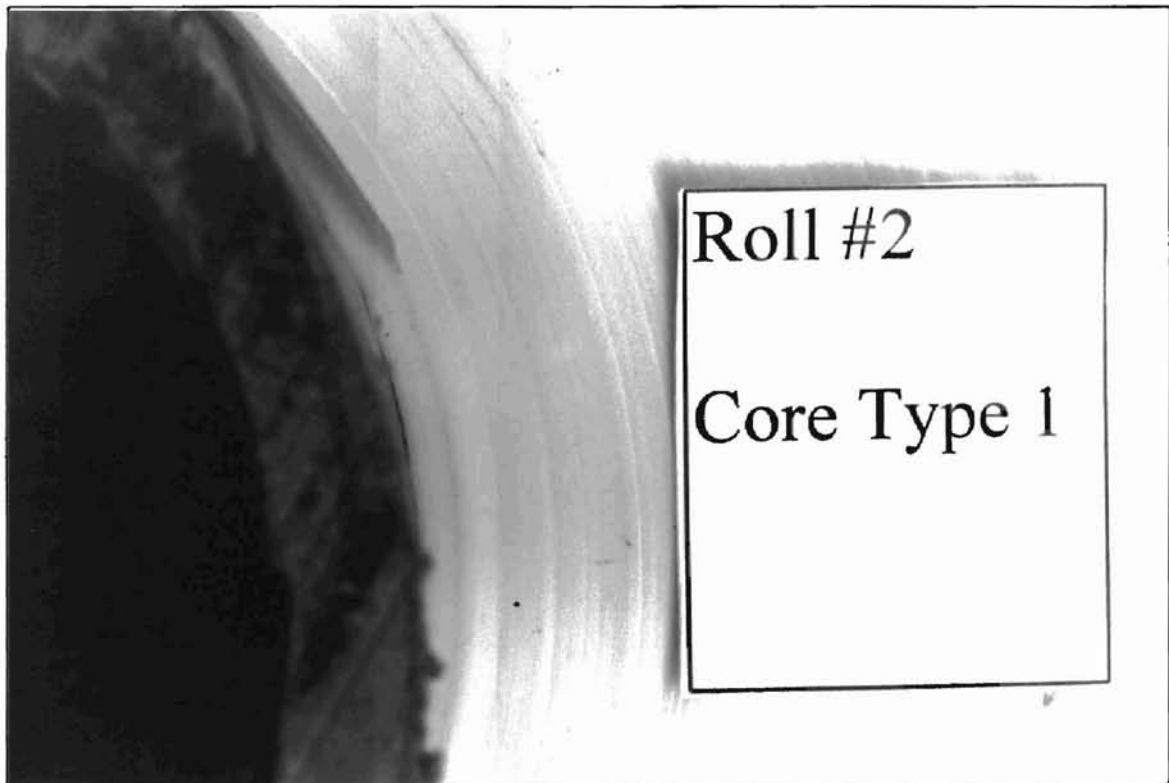


Figure A-4, Roll #2.

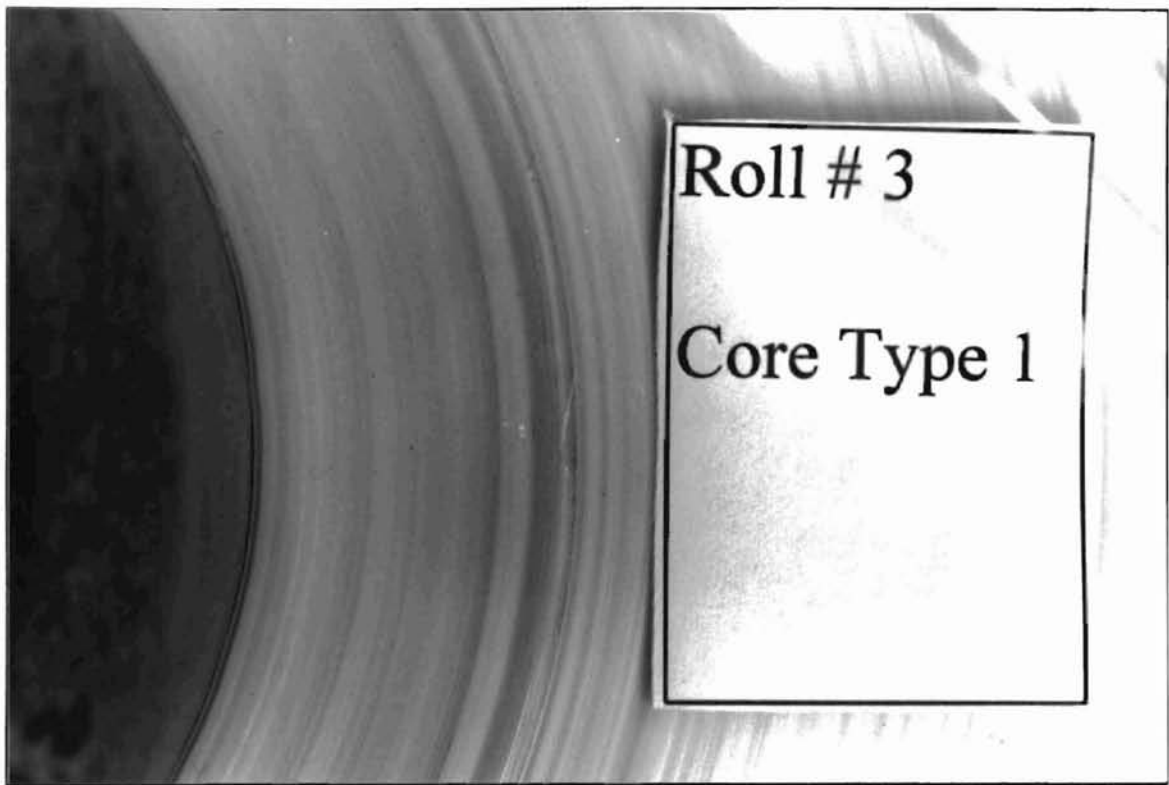


Figure A-5, Roll #3.

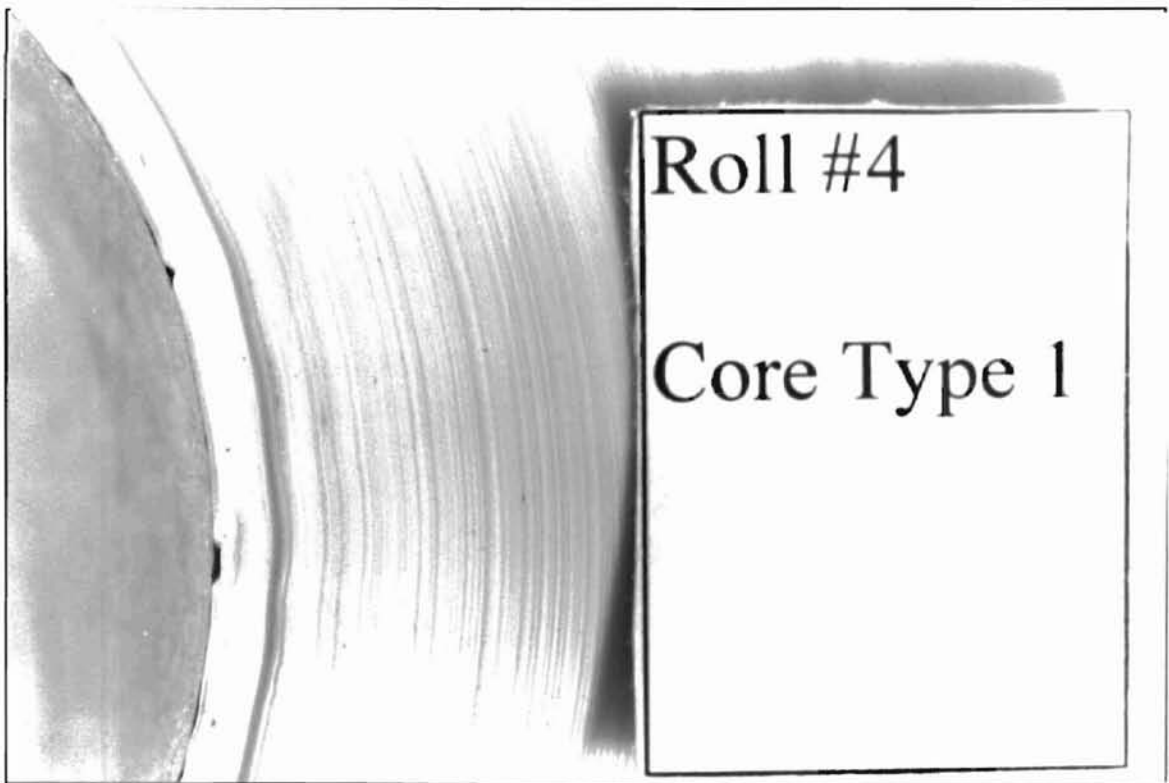


Figure A-6 Roll # 4.

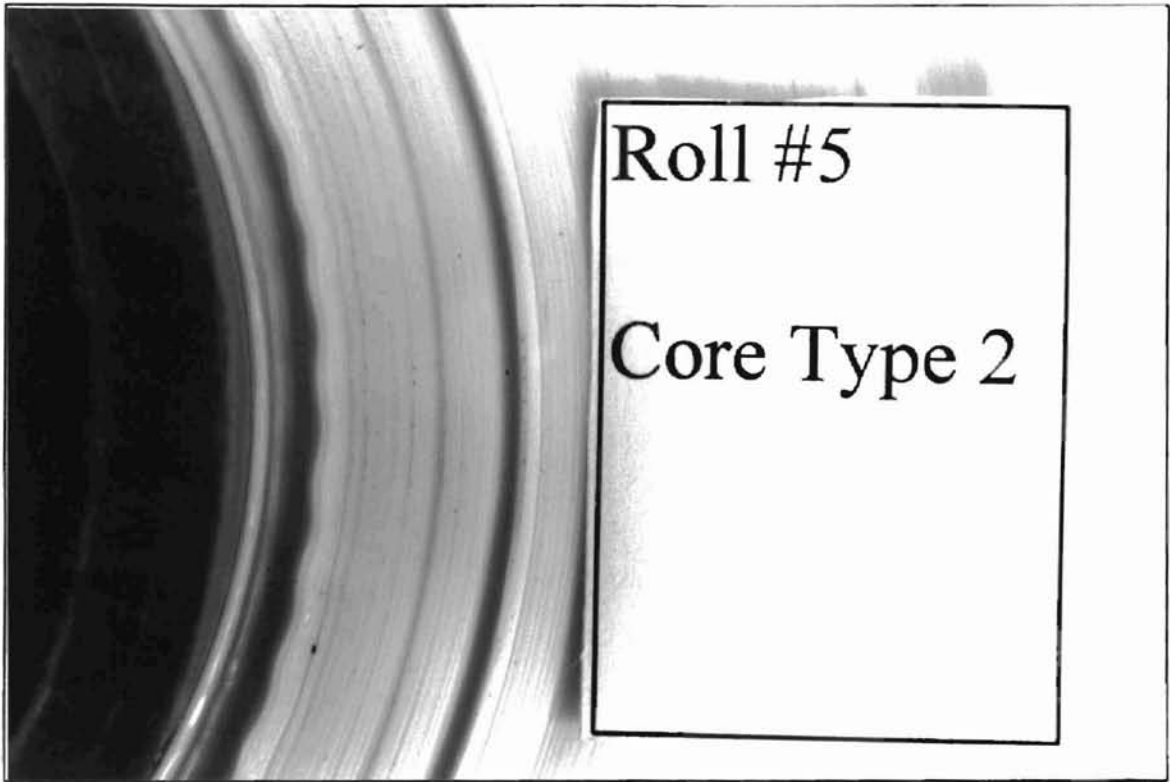


Figure A-6 Roll # 5.

APPENDIX B  
COMPUTER CODE

```

*****
*****
*****
*****
***** CORE RELAXATION *****
***** 1st ed. *****
***** Written By: Jeff Henning *****
***** Project Coordinator: Dr. J. Keith Good *****
*****
***** Web Handling Research Laboratory (WHRC) *****
***** Oklahoma State University *****
***** Department of Mechanical and Aerospace Engineering *****
***** Stillwater, Oklahoma *****
*****
***** Calculates Stresses Induced Due to the *****
***** Relaxation of the Core in Time *****
***** *****
*****
*****
*****
**
***** Main Program Corerelax
***** -opens and closes input/output files
***** -make calls to subroutine
**
*****
PROGRAM CORERELAX
OPEN(1,FILE='CORECRP.IN')
OPEN(2,FILE='CORECRP.OUT')
OPEN(4,FILE='COREPRS.OUT')
WRITE(*,*)'*****'
WRITE(*,*)'ENTER "1" FOR FILE INPUT OR "0" FOR KEYBOARD INPUT'
READ(*,*)IANS
WRITE(*,*)'*****'
IF(IANS.EQ.0) THEN
CALL UINPUTS
ELSE
CALL INPUTS
ENDIF
WRITE(4,120)
WRITE(*,*)'*****Calculating*****'
CALL WINDER
CALL RELAX
WRITE(*,*)'*****Finished*****'
WRITE(*,*)'*****'

```

```

C  CALL OUTS
120 FORMAT('  TIME      PRESSURE  DELTA      B(1)')
      CLOSE(2)
      CLOSE(4)
      STOP
      END
*****
*****
**
**** Subroutine RELAX
*****
      SUBROUTINE RELAX
      IMPLICIT REAL*8 (A-H,J,O-Z)
      COMMON/PARAM/RINC,RIN,ROUT,NLAPS,NINC,NCORE,WT
      COMMON/CLOCK/DCLOCK,U(1000),DTP(1000),NCLOCK,J0,J1,T1,J2,T2
      COMMON/MATLPROP/EC,E,vc,ET,AA(0:3),ER(1000),vrt,vtr
      COMMON/TIME/R(1000),TIME,TWIND,LAP,DTOLD,DTIME
      COMMON/MATCOEFF/A(1000),B(1000),C(1000),D(1000),N
      COMMON/PRES/P(1000),DP(1000),S,OLDP,VP(1000)
C  WRITE(*,*)'THSTRESS IN OK'
C
C
C
C
      R(1)=RIN
      LAP=1
      H=(ROUT-RIN)/NLAPS
      DO I=2,NLAPS+1
      R(I)=R(1)+(I-1)*H
      END DO
C
C
C
C
      DO L=1,NLAPS
      VP(L)=P(L)
      END DO
C
      DCLOCK=DCLOCK/NCLOCK
      DO 999 K=1,NCLOCK
      TIME=K*DCLOCK
      WRITE(2,100)TIME
C
C
C
cccccccccccccccccccccccccccccccccccccccc
CCCC THIS IS STRESS FORMULATION WITH EC
C
CCC CORE BOUNDARY CONDITION

```

```

C
D(1)=(1D0-vrt-Et/(Ec*RIN)-RIN/H)
C D(1)=(1d0-Et/Er(1)*vtr-Et/(Ec*rin))
C(1)=rin/h
S=-P(1)
OLDP=-P(1)
B(1)=Et*S*(J0+J1*EXP(-TIME/T1)+J2*EXP(-TIME/T2))
C
CCC ROLL ANALISIS
C
DO 60 I=2, NLAPS
vtr=vrt*Er(I)/Et
A(I-1)=(R(I)**2/H**2-R(I)/(2D0*H)*(3d0-Et/Er(I)*vtr+vrt))
D(I)=(1D0-2D0*R(I)**2/H**2+vrt-Et/Er(I)*(1+vtr))
C(I)=R(I)**2/H**2+R(I)/(2D0*H)*(3d0-Et/Er(I)*vtr+vrt)

C A(I-1)=(R(I)**2/H**2-3D0*R(I)/(2D0*H))
C D(I)=(1D0-2D0*R(I)**2/H**2-Et/Er(I))
C C(I)=R(I)**2/H**2+3D0*R(I)/(2D0*H)
C
B(I)=0D0
C
60 CONTINUE
C
CCC OUTER BOUNDARY CONDITION
C
D(NLAPS+1)=1D0
B(NLAPS+1)=0D0
A(NLAPS)=0D0
C
C
CCC SOLVE MATRIX FOR PRESSURES AND PRINT
C
CALL SOLVETRI(DTP,NLAPS+1)
LAP=NLAPS+1
CALL VTOTPRESS(DTP)
CALL OUTS
C CALL STRAIN
999 CONTINUE
C
100 FORMAT('TIME =',F7.0,' (MIN)')
C WRITE(*,*)'THSTRESS OUT OK'
RETURN
END
*****

```

```

*****
****Subroutine Strain
****Solves the strain at the first layer of roll
**** which is equal to the strain of the core
*****

```

```

SUBROUTINE STRAIN
IMPLICIT REAL*8 (A-H,J,O-Z)
COMMON/PARAM/RINC,RIN,ROUT,NLAPS,NINC,NCORE,WT
COMMON/CLOCK/DCLOCK,U(1000),DTP(1000),NCLOCK,J0,J1,T1,J2,T2
COMMON/MATLPROP/EC,E,vc,ET,AA(0:3),ER(1000),vrt,vtr
COMMON/TIME/R(1000),TIME,TWIND,LAP,DTOLD,DTIME
COMMON/MATCOEFF/A(1000),B(1000),C(1000),D(1000),N
COMMON/PRES/P(1000),DP(1000),S,OLDP,VP(1000)
COMMON/STRN/VSTRN,ESTRN,TSTRN

C  WRITE(*,*)'STRAIN IN OK'
C  VSTRN=VSTRN+((J0+J1*EXP(-TIME/T1)+J2*EXP(-TIME/T2))*OLDP)
C  ' *1000000)
  VSTRN=VSTRN+B(1)
  ESTRN=(P(1)/EC)*1000000
  TSTRN=(VSTRN+ESTRN)
C  WRITE(3,40)
C  WRITE(3,50)TIME,TSTRN,VSTRN,ESTRN
50  FORMAT(F10.2,' ',F15.4,' ',F15.4,' ',F10.4)
  RETURN
  END

```

```

*****
*****
**** Subroutine SOLVETRI
**** -SOLVES THE TRIDIAGONAL SYSTEM OF DIMENSION IDIM
**** FOR THE SOLUTION VECTOR X(IDIM)
*****

```

```

SUBROUTINE SOLVETRI(X,IDIM)
IMPLICIT REAL*8 (A-H,J,O-Z)
INTEGER IDIM
DIMENSION X(1000)
COMMON/MATCOEFF/A(1000),B(1000),C(1000),D(1000),N
C  WRITE(*,*)'SOLVE IN OK '
  N=IDIM
  DO 900 I=2,N
    D(I)=D(I)-(A(I-1)/D(I-1))*C(I-1)
    B(I)=B(I)-(A(I-1)/D(I-1))*B(I-1)
900  CONTINUE
  X(N)=B(N)/D(N)
  DO 910 I=(N-1),1,-1

```



```

      X(I)=(B(I)-C(I)*X(I+1))/D(I)
910 CONTINUE
C   WRITE(*,*)'SOLVETRI OUT OK '
      RETURN
      END
*****
*****
***** Subroutine TOTPRESS
***** -UPDATES THE TOTAL PRESSURE P(I)
***** -UPDATES THE INITIAL VISCOELASTIC CHANGE IN PRESSURE VDP(I)
***** -UPDATES THE INITAL TOTAL VISCOELASTIC CHANGE IN PRESSURE
VP(I)
*****
      SUBROUTINE VTOTPRESS(DELTA)
      IMPLICIT REAL*8 (A-H,J,O-Z)
      DIMENSION DELTA(1000)
      COMMON/PARAM/RINC,RIN,ROUT,NLAPS,NINC,NCORE,WT
      COMMON/MATLPROP/EC,E,vc,ET,AA(0:3),ER(1000),vrt,vtr
      COMMON/TIME/R(1000),TIME,TWIND,LAP,DTOLD,DTIME
      COMMON/PRES/P(1000),DP(1000),S,OLDP,VP(1000)
C
      DO I=1,LAP
      P(I)=P(I)+DELTA(I)
      Er(I)=AA(3)*(ABS(P(I)))**3+AA(2)*(ABS(P(I)))**2+AA(1)*
' (ABS(P(I))+AA(0)
      END DO
C
      RETURN
      END
*****
*****
***** Subroutine OUTS
***** -PRINTS OUPUT OF RADIAL PRESSURES TO THE FILE "OUT.DAT"
*****
      SUBROUTINE OUTS
      IMPLICIT REAL*8 (A-H,J,O-Z)
      COMMON/PARAM/RINC,RIN,ROUT,NLAPS,NINC,NCORE,WT
      COMMON/CLOCK/DCLOCK,U(1000),DTP(1000),NCLOCK,J0,J1,T1,J2,T2
      COMMON/MATCOEFF/A(1000),B(1000),C(1000),D(1000),N
      COMMON/MATLPROP/EC,E,vc,ET,AA(0:3),ER(1000),vrt,vtr
      COMMON/TIME/R(1000),TIME,TWIND,LAP,DTOLD,DTIME
      COMMON/PRES/P(1000),DP(1000),S,OLDP,VP(1000)
C
C
C   WRITE(*,*)'OUTS IN OK '

```

```

      PHRASE='*****'
      WRITE(2,20) RADIUS      PRESSURE      DELTA'
C     WRITE(5,60)TIME
      DO 9200 I=1,NLAPS+1
      WRITE(2,30)R(I),P(I),DTP(I)
9200 CONTINUE
      WRITE(4,40)TIME,P(1),DTP(1),B(1)
C
10  FORMAT(1X,A50)
20  FORMAT(A47,' ',F10.1)
30  FORMAT(F15.4,' ',F15.8,' ',E15.8)
40  FORMAT(F10.0,' ',F15.4,' ',E15.8,' ',E15.8)
      RETURN
      END
*****
*****
***** Subroutine INPUTS
***** -INITIALIZES ALL INPUTS PARAMETERS BY READING
***** INPUT FILE "IN.DAT"
*****
      SUBROUTINE INPUTS
      IMPLICIT REAL*8 (A-H,J,O-Z)
      COMMON/PARAM/RINC,RIN,ROUT,NLAPS,NINC,NCORE,WT
      COMMON/CLOCK/DCLOCK,U(1000),DTP(1000),NCLOCK,J0,J1,T1,J2,T2
      COMMON/MATLPROP/EC,E,vc,ET,AA(0:3),ER(1000),vtr,vtr
CCC
C     WRITE(*,*)'ENTER THE WINDING TENSION '
      READ(1,100)WT
C     WRITE(*,*)'ENTER THE INSIDE RADIUS OF THE CORE '
C     READ(1,100)RINC
C     WRITE(*,*)'ENTER THE INSIDE RADIUS OF THE ROLL '
      READ(1,100)RIN
C     WRITE(*,*)'ENTER THE OUTSIDE RADIUS OF THE ROLL '
      READ(1,100)ROUT
C     WRITE(*,*)'ENTER THE RADIAL STIFFNESS OF THE CORE '
      READ(1,120)EC
C     WRITE(*,*)'ENTER THE YOUNGS MODULUS OF THE CORE '
C     READ(1,120)E
C     WRITE(*,*)'ENTER POISSONS RATIO OF THE CORE '
      READ(1,100)vc
C     WRITE(*,*)'ENTER THE TANGENTIAL MODULUS OF THE ROLL'
      READ(1,100)ET
C     WRITE(*,*)'ENTER THE COEFFICIENTS (c3,c2,c1,c0) OF THE '
C     WRITE(*,*)'RADIAL MODULUS  $ER=c3*P^2+c2*P+c1*P+c0$  '
      READ(1,120)AA(3),AA(2),AA(1),AA(0)

```

```

C  WRITE(*,*)'ENTER THE POISSONS RATIO vrt OF THE ROLL'
  READ(1,100)vrt
C  WRITE(*,*)'ENTER THE POISSONS RATIO vtr OF THE ROLL'
  READ(1,100)vtr
C
  READ(1,120)J0
C
  READ(1,120)J1
C
  READ(1,120)T1
C
  READ(1,120)J2
C
  READ(1,120)T2
C
C  WRITE(*,*)'ENTER THE TOTAL NUMBER OF LAPS TO BE WOUND '
  READ(1,110)NLAPS
C  WRITE(*,*)'ENTER NUMBER OF CORE SEGMENTS (FOR DISPL FORM)'
C  READ(1,110)NCORE
C  WRITE(*,*)'ENTER THE CHANGE IN TIME '
  READ(1,100)DCLOCK
C  WRITE(*,*)'ENTER THE NUMBER TIME INCREMENTS'
  READ(1,110)NCLOCK
100 FORMAT(F12.4)
110 FORMAT(I9)
120 FORMAT(E12.5)
  CLOSE(1)
130 continue
  RETURN
  END
*****
*****
***** Subroutine UINPUTS
***** -INITIALIZES ALL INPUTS PARAMETERS BY READING
***** KEYBOARD ENTRY
*****
  SUBROUTINE UINPUTS
  IMPLICIT REAL*8 (A-H,J,O-Z)
  COMMON/PARAM/RINC,RIN,ROUT,NLAPS,NINC,NCORE,WT
  COMMON/CLOCK/DCLOCK,U(1000),DTP(1000),NCLOCK,J0,J1,T1,J2,T2
  COMMON/MATLPROP/EC,E,v,ET,AA(0:3),ER(1000),vrt,vtr
CCC
  WRITE(*,*)'ENTER THE WINDING TENSION '
  READ(*,100)WT
  WRITE(1,100)WT

```

```

C  WRITE(*,*)'ENTER THE INSIDE RADIUS OF THE CORE '
C  READ(*,100)RINC
C  WRITE(1,100)RINC
  WRITE(*,*)'ENTER THE INSIDE RADIUS OF THE ROLL '
  READ(*,100)RIN
  WRITE(1,100)RIN
  WRITE(*,*)'ENTER THE OUTSIDE RADIUS OF THE ROLL '
  READ(*,100)ROUT
  WRITE(1,100)ROUT
  WRITE(*,*)'ENTER THE RADIAL STIFFNESS OF THE CORE '
  READ(*,120)EC
  WRITE(1,120)EC
C  WRITE(*,*)'ENTER THE YOUNGS MODULUS OF THE CORE '
C  READ(*,120)E
C  WRITE(1,120)E
  WRITE(*,*)'ENTER POISSONS RATIO OF THE CORE '
  READ(*,100)vc
  WRITE(1,100)vc
  WRITE(*,*)'ENTER THE TANGENTIAL MODULUS OF THE ROLL'
  READ(*,100)ET
  WRITE(1,100)ET
  WRITE(*,*)'ENTER THE COEFFICIENTS (c3,c2,c1,c0) OF THE '
  WRITE(*,*)'RADIAL MODULUS  $ER=c3*P^3+c2*P^2+c1*P+c0$  '
  READ(*,120)AA(3),AA(2),AA(1),AA(0)
  WRITE(1,120)AA(3),AA(2),AA(1),AA(0)
  WRITE(*,*)'ENTER THE POISSONS RATIO  $\nu_{rt}$  OF THE ROLL'
  READ(*,100) $\nu_{rt}$ 
  WRITE(1,100) $\nu_{rt}$ 
  WRITE(*,*)'ENTER THE POISSONS RATIO  $\nu_{tr}$  OF THE ROLL'
  READ(*,100) $\nu_{tr}$ 
  WRITE(1,100) $\nu_{tr}$ 
  WRITE(*,*)'ENTER THE CREEP FUNCTION COEFFICIENTS'
  WRITE(*,*)' $J=J_0+J_1*EXP(-t/T_1)+J_2*EXP(-t/T_2)$ '
  WRITE(*,*)'J0'
  READ(*,120)J0
  WRITE(1,120)J0
  WRITE(*,*)'J1'
  READ(*,120)J1
  WRITE(1,120)J1
  WRITE(*,*)'T1'
  READ(*,120)T1
  WRITE(1,120)T1
  WRITE(*,*)'J2'
  READ(*,120)J2
  WRITE(1,120)J2

```

```

WRITE(*,*)'T2'
READ(*,120)T2
WRITE(1,120)T2
WRITE(*,*)'ENTER THE TOTAL NUMBER OF LAPS TO BE WOUND < 1000'
READ(*,110)NLAPS
WRITE(1,110)NLAPS
C  WRITE(*,*)'ENTER NUMBER OF CORE SEGMENTS (FOR DISPL FORM)'
C  READ(*,110)NCORE
C  WRITE(1,110)NCORE
WRITE(*,*)'ENTER THE CHANGE IN TIME '
READ(*,100)DCLOCK
WRITE(1,100)DCLOCK
WRITE(*,*)'ENTER THE NUMBER TIME INCREMENTS'
READ(*,110)NCLOCK
WRITE(1,110)NCLOCK
100 FORMAT(F12.4)
110 FORMAT(I9)
120 FORMAT(E12.5)
CLOSE(1)
130 continue
RETURN
END

```

```

*****
*****
**

```

```

***** Subroutine Winder
***** -similar to standard elastic finite difference winding routines
***** -determines the change in radial pressure at radial increment
***** due to the addition of each layer
***** -store these values in the array DP(layer,layer)
**

```

```

*****

```

```

SUBROUTINE WINDER
IMPLICIT REAL*8 (A-H,J,O-Z)
COMMON/PARAM/RINC,RIN,ROUT,NLAPS,NINC,NCORE,WT
COMMON/CLOCK/DCLOCK,U(1000),DTP(1000),NCLOCK,J0,J1,T1,J2,T2
COMMON/MATLPROP/EC,E,vc,ET,AA(0:3),ER(1000),vrt,vtr
COMMON/TIME/R(1000),TIME,TWIND,LAP,DTOLD,DTIME
COMMON/MATCOEFF/A(1000),B(1000),C(1000),D(1000),N
COMMON/PRES/P(1000),DP(1000),S,OLDP,VP(1000)
COMMON/TRY/AA1,BB1,CC1,RK

```

```

C
CCCCC CALCULATE INITIAL PRESSURES
C
C  WT=100.0

```

```

C   Ec=E*(rin**2-rinc**2)/(rin**2+rinc**2-vc*(rin**2-rinc**2))/rin
C
C   WRITE(*,*)'WINDER IN OK'
      H=(ROUT-RIN)/NLAPS
      R(1)=RIN
      LAP=1
      DO I=2,NLAPS+1
        R(I)=R(1)+(I-1)*H
      END DO
C
CCCCC WIND FIRST LAP
C   WRITE(*,*)'ONE'
C
      LAP=1
      DT=EC*WT*RIN**2/(EC*R(1)**2+H*ET)
      DT=WT
      DP(1)=(-DT*H)/R(1)
      CALL TOTPRESS(DP)

C
CCCCC WIND ON SECOND LAP
C
C   WRITE(*,*)'TWO'
      LAP=LAP+1
      I=LAP
      D(1)=(1D0-vrt-Et/(Ec*RIN)-RIN/H)
      C(1)=R(1)/H
      B(1)=0D0
      DP(2)=(-WT*H)/R(LAP)
      DP(1)=(B(1)-DP(2)*C(1))/D(1)
      CALL TOTPRESS(DP)

c
CCCCC WIND ON ALL REMAINING LAPS
C
      DO 50 M=3,NLAPS
        LAP=M
C
        D(1)=1D0-vrt-Et/(Ec*RIN)-RIN/H
        C(1)=R(1)/H
        B(1)=0D0
C
        DO I=2, LAP-1
          A(I-1)=(R(I)**2/H**2-3D0*R(I)/(2D0*H))
          D(I)=(1D0-2D0*R(I)**2/H**2-Et/Er(I))
          C(I)=R(I)**2/H**2+3D0*R(I)/(2D0*H)

```

```

      B(I)=0D0
      END DO
C
      DP(LAP)=(-WT*H)/R(LAP)
      B(LAP)=DP(LAP)
      D(LAP)=1D0
      A(LAP-1)=0D0
C
C
      CALL SOLVETRI(DP,LAP)
      CALL TOTPRESS(DP)
50  CONTINUE
      CALL OUTS
C   WRITE(*,*)'WINDER OUT OK'
      RETURN
      END
*****
*****
***** Subroutine TOTPRESS
***** -UPDATES THE TOTAL PRESSURE P(I)
***** -UPDATES THE INITIAL VISCOELASTIC CHANGE IN PRESSURE VDP(I)
***** -UPDATES THE INITIAL TOTAL VISCOELASTIC CHANGE IN PRESSURE
VP(I)
*****
      SUBROUTINE TOTPRESS(DELTA)
      IMPLICIT REAL*8 (A-H,J,O-Z)
      DIMENSION DELTA(1000)
      COMMON/PARAM/RINC,RIN,ROUT,NLAPS,NINC,NCORE,WT
      COMMON/MATLPROP/EC,E,vc,ET,AA(0:3),ER(1000),vrt,vtr
      COMMON/TIME/R(1000),TIME,TWIND,LAP,DTOLD,DTIME
      COMMON/PRES/P(1000),DP(1000),S,OLDP,VP(1000)
C
      DO I=1,LAP
      P(I)=P(I)+DELTA(I)
      Er(I)=AA(3)*(ABS(P(I)))**3+AA(2)*(ABS(P(I)))**2+AA(1)*
' (ABS(P(I)))+AA(0)
      END DO
C
      RETURN
      END

```

VITA

Jeffrey Scott Henning

Candidate for the Degree of

Master of Science

Thesis: EFFECTS OF RELAXATION OF A CORE ON A WOUND ROLL

Major Field: Mechanical Engineering

Biographical:

Personal Data: Born in Stillwater, Oklahoma, on August 24, 1966. Married to Rebecca Sue Worsham.

Education: Graduated from Jenks High School, Jenks, Oklahoma, in May 1984; attended Oral Roberts University and Tulsa Community College; received Bachelor of Science degree in Mechanical Engineering from Oklahoma State University, Stillwater, Oklahoma, in May 1995. Completed the requirements for the Master of Science degree with a major in Mechanical Engineering at Oklahoma State University in May, 1997.

Experience: Employed in industry before returning to finish degree. Research Assistant at the OSU Web Handling Research Center.

Professional Memberships: Oklahoma Society of Professional Engineers, National Society of Professional Engineers, Certified Engineer Intern.